THE DESIGN, DEVELOPMENT, FABRICATION AND TESTING OF A 100 WATT SKUTTERUDITE THERMOELECTRIC GENERATOR

By

Matthew Lyle

A THESIS

Submitted to
Michigan State University
in partial fulfillment of the requirements
for the degree of

MASTER OF SCIENCE

Mechanical Engineering

2011

ABSTRACT

THE DESIGN, DEVELOPMENT, FABRICATION AND TESTING OF A 100 WATT SKUTTERUDITE THERMOELECTRIC GENERATOR

By

Matthew Lyle

Thermoelectric technology is a method of renewable, alternative energy that utilizes the Seebeck effect to convert some of the thermal energy in a temperature gradient to electricity. The optimal temperature range for skutterudite thermoelectric devices is around 650°C, making them ideal for high temperature applications. At this temperature range, the skutterudite thermoelectrics have a device-level conversion efficiency of about 9% [1]. As these devices are still in the development stage, testing that simulates real-world conditions is necessary to assess the feasibility of implementing skutterudite thermoelectric technology with current processes.

A standardized procedure to test the skutterudite thermoelectric devices has been established to reduce variability in device fabrication and generator assembly. This procedure includes a measurement and tracking system to aid in establishing relationships between component properties and thermoelectric performance. In addition, a technology has been developed to electrically bypass any failed devices to preserve overall power generation.

Results indicate that additional efforts are needed to address the high level of thermal stresses the devices experience during operation. Several methods to reduce thermal stresses and investigate potential stressors are proposed. In addition, the successful performance of the electrical bypass technology suggests that it is indeed a viable method of bypassing individual devices for experimental tests. Additional testing and improvements can be made as necessary to implement this technology in the envisioned 1 kW skutterudite thermoelectric generator.

ACKNOWLEDGEMENTS

The discoveries and accomplishments detailed in this Thesis are the result of hard work, continual support and expert guidance from a number of individuals. I would like to first and foremost thank my advisor, Dr. Harold Schock who believed in me from our first meeting and has shown nothing but support and encouragement during my time at MSU. In addition, his solid methodology and perceptive insights shared during the course of this project have been instrumental in addressing critical problems and determining next steps.

I would also like to thank my colleagues at MSU who have worked me on this project, shared their expertise and included me as a friend. First of all, Trevor Ruckle, who spearheaded the module design and created the generator design and the testing process, has taken me under his wing for the past 2 years and has tirelessly answered my many questions, saved me from countless mistakes and has redefined the meaning of “Practical Wisdom.” Dr. Jeff Sakamoto, who invented the individual couple testing procedure and Ryan Maloney have both made significant contributions in effectively integrating the aerogel insulation technology with the thermoelectric devices as well as providing an in-depth analysis and explanation of the material interactions from a material science perspective. Edward Timm, who created the flexible hot shoe design, and Dr. Long Zhang have both devoted substantial efforts to material synthesis and testing and have also identified and implemented improvements to the fabrication and testing processes, as well as to the material itself. Kevin Moran and Timothy Stewart developed the Couple Bypass Technology and have made substantial, ongoing improvements to its design and control. Dr. George Zhu has also played a prominent role in drafting electronic designs and highlighting electrical considerations. Finally, Jeff Higel and Gary Keeney have performed exceptional machining work for this project and have gone out of their way to make me feel welcome here at MSU.

I would like to thank my parents, Stephen and Katrina Lyle for their support and guidance over the course of my life. They have always been willing to lend a hand, offer advice, or simply be a listening ear. My sister, Rebecca and my brother, Daniel have also encouraged me, believed in me and have both taught me invaluable life lessons that I will never forget.

The incredible support and encouragement that my wife, Katie, has shown me during this journey has entrenched in me a commitment for excellence and a grateful appreciation for the best life partner I could ever have hoped for.

Finally, and most importantly, I would like to thank my Lord and Savior, Jesus Christ, without whom, I am truly less than nothing.

TABLE OF CONTENTS

LIST OF TABLES

LIST OF FIGURES

LIST OF SYMBOLS AND ACRONYMS

ΔT	Change in Temperature
°	Degree
μm	Micrometer
AWG	American Wire Gauge
Ba	Barium
C	Celsius
CAN	Controller Area Network
CBT	Couple Bypass Technology
Ce	Cerium
CFH	Cubic Feet per Hour
CFM	Cubic Feet per Minute
cm	Centimeter
Co	Cobalt
CTE	Coefficient of Thermal Expansion
EAS	Electrically Activated Switch
ERS-APU	Energy Recovery System - Auxiliary Power Unit
Fe	Iron
FR	Flame Retardant
FEA	Finite Element Analysis
gal	Gallon
I	Current
kg	Kilogram

kPa	Kilopascal
kW	Kilowatt
MJ	Megajoule
ml	Milliliter
mm	Millimeter
mV	Millivolt
MPG	Miles per Gallon
MSU	Michigan State University
OTR	Over the Road
P	Power
R_{EAS}	Resistance across EAS
rpm	Revolutions per Minute
RTG	Radioisotope Thermoelectric Generator
Sb	Antimony
Sn	Tin
TE	Thermoelectric
TED	Thermoelectric Device
TEG	Thermoelectric Generator
V	Volt
V_{AL}	EAS Activation-Signal-to-Low-Side Voltage
W	Watt
Yb	Ytterbium

Chapter 1

1. Introduction

The entropy generation that prevents processes from being reversible is often caused in part by waste heat. Opportunities to improve the overall efficiency of these processes can be realized by converting some of the energy in the waste heat to useful work. As industry standards and governmental regulations become more aggressive, this opportunity becomes even more appealing. In addition, accurately identifying and implementing viable sources of renewable, alternative energy is necessary to lessen global dependence on fossil fuels and establish a system of sustainable energy production.

1.1. TE Overview

Thermoelectric (TE) technology is one area of waste heat energy recycling that has received renewed interest in the last few decades. Thermoelectric Devices (TEDs) utilize the Seebeck effect to convert some of the thermal energy in a temperature gradient to electricity. Much progress has already been made with low temperature thermoelectric generators (TEGs) and several variations of low temperature TEGs made from materials such as bismuth telluride are currently being manufactured and sold. Recently, research efforts have focused more heavily on non-heritage, high temperature thermoelectric generators, which feature significant benefits but also greater challenges. High temperature TEGs open the door to a wider range of applications than low temperature TEGs alone. However, the higher operating temperatures of these devices incur higher levels of thermal stresses, placing the thermoelectric components at higher risk of structural failure. Mitigating this risk is necessary to produce durable, reliable, high temperature TEGs that can undergo several thermal cycles without significant degradation.

1.1.1. History

In 1821 AD, Thomas Johann Seebeck discovered that a compass magnet could be deflected by joining two dissimilar metals in a circuit and exposing the junctions to different temperatures. It was later realized that this magnet deflection was induced by an electric current in the circuit. This effect was further investigated and explained by Jean-Charles Peltier, who discovered that an electrical current would heat or cool the junctions of the circuit, and by William Thomson (Lord Kelvin) who summarized that a given material exposed to a temperature gradient will either absorb or release heat when subjected to an electrical current [2-3].

Thermoelectrics have played a prominent role in NASA's Radioisotope thermoelectric generators (RTGs) which have powered several exploratory spacecraft such as Voyager 1 and Voyager 2 [4-6]. RTGs have also been used for some terrestrial applications, including lighthouses and navigation beacons [7]. The terrestrial applications for RTGs have been limited, due to the low system efficiencies and the inherent risk associated with using radioactive materials for the heat source. Recently, however, advances in material science and a greater push for "green" energies have sparked a renewed interest in thermoelectric technology, particularly for the automotive industry, which is facing ever-tightening fuel economy and emissions regulations.

1.1.2. How TEDs work

Modern TE technology utilizes the discoveries made by Seebeck, Peltier and Lord Kelvin to convert some of the thermal energy in a temperature gradient to electricity. Materials that drive current *toward* the hot side when exposed to a temperature gradient are referred to as N-type, whereas materials that drive current *away* from the hot side are referred to as P-type. Joining the hot sides of an N-type material and a P-type material creates a thermoelectric circuit, able to power a load between the cold sides of the two materials (Figure 1-1). This unit is commonly referred to as a thermoelectric couple. Combining several of these couples in series allows for greater power values.

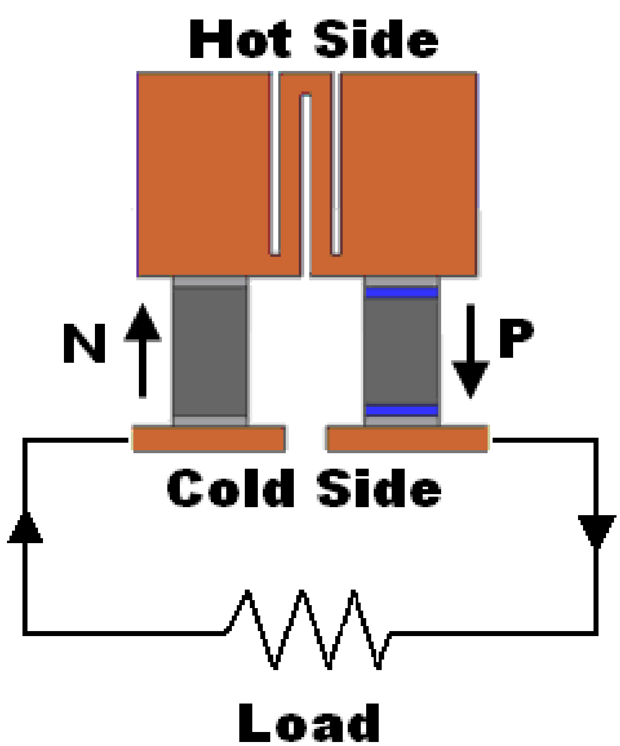

Figure 1-1 Thermoelectric Couple

There are several other technologies that exist to convert waste heat into useful work, including steam turbines and Sterling engines. Compared to these competing technologies, thermoelectrics have several advantages, including:

- High reliability (>250,000 hours)
- Silent operation
- No vibration
- Small electromagnetic signature
- Precise temperature control (fractions of a degree)
- Position independent
- Small and lightweight
- Environmentally “green”
- Direction of heat pumping is fully reversible
- No chlorofluorocarbons, chemicals or compressed gases (nothing to replenish)
- Able to function in environments too severe or sensitive for conventional refrigeration

However, it should also be noted that current thermoelectric technology has lower efficiencies compared to competing technologies [8].

1.2. Project Scope

Much of the research in the thermoelectrics area has been devoted to synthesizing and testing various thermoelectric materials. This is a rather appropriate place to focus initial research efforts, as the thermal and electrical properties of the TE materials determine the feasibility of producing TEDs on a manufacturing scale. To validate the findings from the materials research, a logical next step is to conduct experiments with the thermoelectric materials that simulate real-world conditions. As well as evaluating the performance of the thermoelectric material, these experiments can also uncover potential roadblocks that may hinder implementation of thermoelectric technology with the present energy infrastructure.

One of the most potentially lucrative applications for TE technology is integration with over-the-road (OTR) trucks. As much as 35% of the energy generated by the vehicle's engine can escape out the tailpipe as waste heat, creating a significant opportunity to reclaim energy [9]. The temperature and flow rate of exhaust gases from OTR trucks provides an ideal heat source and the engine's cooling system can be modified to act as the heat sink. In addition, the high duty cycle and large idling time experienced by most OTR trucks offers a sizable opportunity for energy recovery. Thus, to help simulate real-world conditions for the experiment, the heat source used in these experiments will, as much as practically possible, simulate the exhaust of an engine used in OTR trucks.

The scope of this Thesis is to experimentally evaluate the thermal, electrical and physical properties of the skutterudite TEDs by conducting performance tests that simulate real-world conditions of the potential OTR truck application for TE technology.

1.3. Outline of Thesis

The present chapter introduces the idea of using TE technology to improve process efficiency by means of waste heat recovery. A brief history and explanation of how TEDs work is given, as well as the advantages and disadvantages of competing technologies. In addition the scope of this Thesis is defined.

The second chapter covers previous work that has been done in the area of thermoelectrics. The results of a WAVE simulation of ideal generator location are presented, followed by a projected cost analysis for mass production of skutterudite TEGs. A finite element analysis of the TE legs is reviewed, as well as previous generator tests that have been conducted with the skutterudite material. Lastly, the research questions are posed.

The third chapter describes the fabrication methods for the TEDs. In addition, the measurement and tracking system is explained.

The fourth chapter introduces the Couple Bypass Technology and describes the design used. Fabrication techniques are also discussed, as well as the procedures of integrating the technology with the TEDs.

The fifth chapter details the generator assembly procedure along with the test fixture and instrumentation. The testing process is outlined and the data collection and post-processing methods are discussed.

The sixth chapter covers the results of 100 W test, as well as the details and results of the follow-up insulation comparison test. The results of the Couple Bypass Technology are also presented, along with the results of the individual couple testing.

The seventh chapter highlights the research achievements made and illustrates the implications of the testing results. In addition, specific “next steps” are suggested to continue research efforts in a way that builds on the knowledge gained from these tests. Finally, the research questions posed in chapter two are answered.

Chapter 2

2. Literature Review

Renewed interest in the field of thermoelectrics has led researchers to investigate a host of various thermoelectric topics. This Thesis and the tests described in the following chapters build on the foundation of previous work laid by researchers exploring the more theoretical aspects of thermoelectrics. The topics covered in this chapter are especially relevant to the experiments detailed in this Thesis.

2.1. Previous Work

While thermoelectrics is still a relatively new field, substantial efforts have been devoted to investigating and developing thermoelectric materials, optimizing generator designs and improving the durability of the thermoelectric couple. To guide research and development efforts, a goal has been established to produce a reliable 1 kW skutterudite thermoelectric generator with an efficiency of $\approx$ 10%. To meet that goal, an incremental approach has been adopted. With this approach, a smaller power goal is set. A generator is assembled from the existing couple design and then tested. Results are evaluated and changes are made to the TE couple and generator designs as needed. The generator is tested again and changes from the previous test are noted. This information is used to make further improvements until the generator meets or exceeds the power goal. A new power goal is then set and the generator is scaled up to meet it. This generator scaling often reveals new areas for improvement and the cycle repeats itself. Power goals of 5 W, 25 W and 50 W have been met by previous tests. Previous 100 W tests produced no more than 75 W despite repeated iterations. This prompted a change from the previous square generator design to the new, round generator design (see section 5.1).

In addition to these experiments, simulations have been conducted help guide research efforts in achieving the aggressive goal of producing a reliable, 1 kW TEG. These theoretical studies have helped to predict expected operating conditions, explain couple breakages that occur during operation and provide a realistic benchmark for generator longevity.

2.1.1. Ideal Location

Much work has already been done studying the many factors involved in integrating TEGs into the exhaust system of OTR trucks. One area of particular interest is the effect of generator location in the exhaust system on thermoelectric performance. A simulation was performed at MSU to compare the amount of power generated for three different TEG configurations: one cylinder per TEG unit, three cylinders per TEG unit and six cylinders per TEG unit [10]. This was achieved by using Ricardo WAVE Engine System Performance Simulation software to model a Cummims ISX engine under the three TEG configurations. Table 2-1 below highlights the findings of this study, which predicted that the design that results in the highest amount of TEG heat energy input is the one cylinder per TEG configuration. A greater amount of system heat energy input results in a higher amount of heat energy converted to electrical energy.

Implementing a one cylinder per TEG design validates the power generation goals for this experiment. These results indicate that to achieve a total of 1 kW of thermoelectric power, it is more practical to install six 170 W TEGs, each fed by a different cylinder, rather than one, 1 kW TEG, fed by all six cylinders. Thus, achieving 100 W of thermoelectric power marks a significant milestone in producing a 1 kW TEG system.

Table 2-1 WAVE Simulation Results

Heat Transfer Results			
Configuration (Optimized Geometry)	TEG Energy Input Rate (kW)	Energy Input per Cylinder (kW/Cylinder)	Total TEG Energy Input (kW/Engine)
One Cylinder Per TEG	31.9	31.9	191.4
Three Cylinders Per TEG	50.2	16.7	100.4
Six Cylinders Per TEG	64.5	10.8	64.5

2.1.2. Cost Analysis

As one of the long term goals for skutterudite thermoelectric research is to develop a robust, low-maintenance TEG that can be integrated with current OTR truck engine designs, a comprehensive cost analysis study is necessary to evaluate the feasibility of mass-producing TEGs. Determining the payback period for the generator also serves as a realistic benchmark for longevity and cycle testing. Intuitively, a viable generator design must perform longer than the payback period to validate the financial venture necessary to purchase, install and maintain the TEGs.

A preliminary cost analysis was estimated for two skutterudite TEG sizes: 1 kW and 5 kW [11]. Specific dollar amounts were assigned by dividing the generator into subsystems, evaluating material costs based on an annual production volume of 10,000 units and using standard estimates for material-to-labor cost ratios. Table 2-2 contains the cost estimates for each subsystem for the 1 kW and the 5 kW generator designs.

Table 2-2 Cost Analysis Results

Cost Estimate - Skutterudte TEG							
Generator Size	Electrical Subsystem	TEDs	Module Assembly	Housing	Burner	Cooling Subsystem	Total
1 kW	$943.28	$1,200	$1,124.85	$400	$717	$388.64	**$4,773.77**
5 kW	$4,671.68	$6,000	$5,624.25	$600	$717	$1,663.20	**$19,276.13**

In addition, the payback period was estimated under the following assumptions:

- A 1kW TEG with belt integrated motor-generator is used to convert waste heat to electrical energy
- The cost of diesel fuel is $4/gal and has an energy density of 38.6 MJ/liter
- The OTR truck has the following fuel economies: 5 MPG base, 5.02 MPG with TEG
- The TEG has a 10% electrical energy conversion efficiency
- Vehicle idle consumes 0.8291 gal/hour without TEG versus 0.249 gal/hour with TEG
- Vehicle operates 300 days per year
- Vehicle spends 8.3 hours on road and 8 hours in idle per day
- Vehicle travels 150,000 miles per year

This study found that 120 gallons of fuel would be saved every year from exhaust heat energy recovery and 1,392 gallons of fuel would be saved every year from idle reduction. At $4 a gallon, this translates to a yearly savings of $6,048 per year or $42,336 over the 7 year (≈ 1 million miles) theoretical life of the engine. Similar estimates were made with the 5 kW TEG. As seen in Figure 2-1, the 1 kW generator is estimated to pay for itself within 1 year and the 5 kW generator is estimated to pay for itself within 3 years.

These results have specific implications for this experiment. While the purpose of the test described in this Thesis is to evaluate total power generation, device integrity should not be ignored. Even if the power goals set for this test are met, further design improvements will need to be made if the thermoelectric components being tested fail at a higher rate than mandated by the payback period. In addition, performance tests will need to be conducted to quantify the amount of device degradation that occurs with repeated cycling.

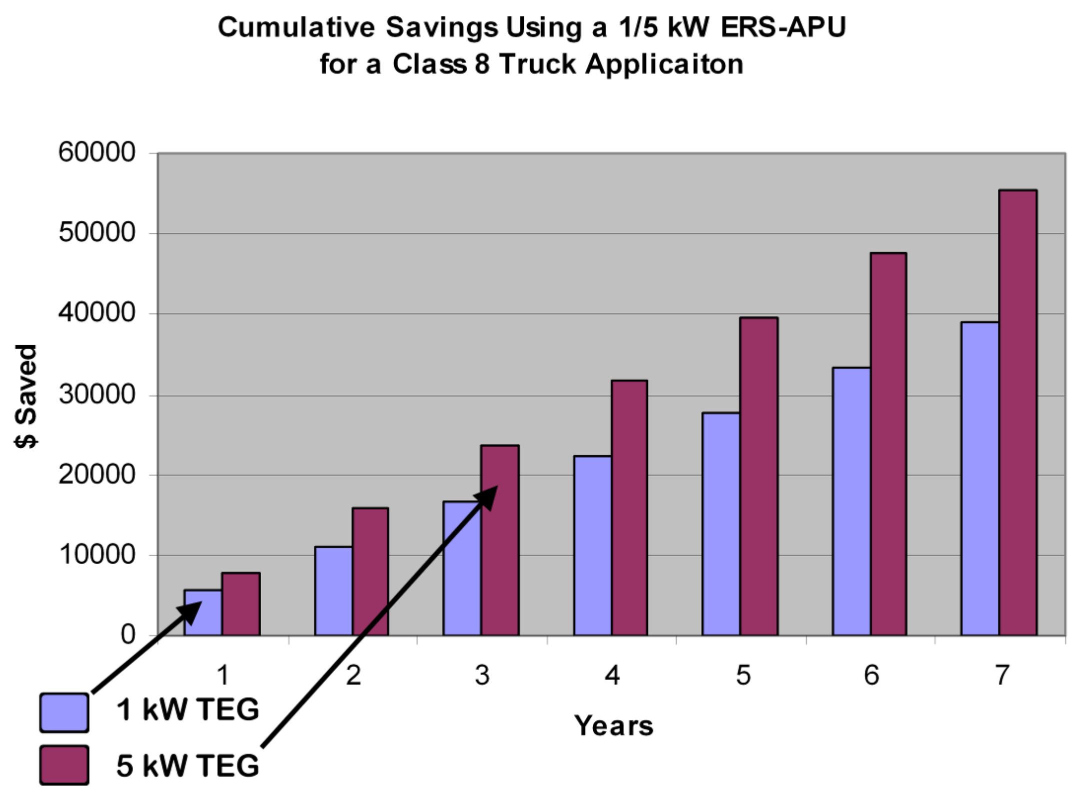

Figure 2-1 Payback Period Estimation

For interpretation of the references to color in this and all other figures, the reader is referred to the electronic version of this Thesis

2.1.3. Finite Element Analysis

The interface between the skutterudite and the metallization layers on the P-type leg (see section 3.2) has been identified as a high-risk area to device durability. This has been confirmed by initial generator power testing which has shown that the most common couple failure mode during operation is a complete material break at the hot-side skutterudite and Material B interface. A finite element analysis (FEA) of the TE couple was conducted at MSU to investigate the effects of thermal cycling on the skutterudite and metallization layer interfaces [12]. A SIMULIA FEA software package, ABAQUS, was used to model the TE couple and simulate thermal cycling. The results of this analysis indicated that the large difference in yield strength between skutterudite and Material B caused the P-type skutterudite to plastically deform when heated, increasing stress levels at the interface. Figure 2-2 shows the stresses on the couple and the bulge between the skutterudite and Material B at operating temperature (about 500°C). Although the stress levels between the metallization layers are higher than those between the skutterudite and Material B, the lower yield strength and ultimate strength of skutterudite makes the skutterudite and Material B interface more vulnerable to failures than the interface between Material A and Material B.

One method of reducing the stress levels at the skutterudite and Material B interface that was proposed in the study was to reduce the cross-sectional area of the TE leg, thereby reducing the amount of material subject to thermal expansion. This proposal was accepted and a smaller leg design that featured half the cross-sectional area of the previous leg design was implemented for this experiment.

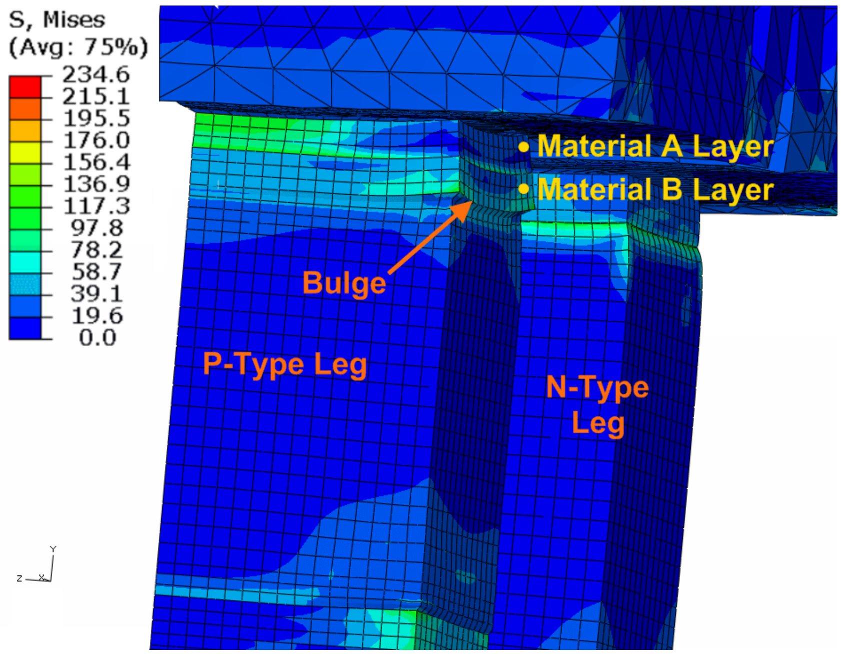

Figure 2-2 FEA Simulation of TE Couple

2.2. Previous Tests

While these topics all relate to skutterudite TEDs, their results are all based on simulations and estimations rather than experiments. To verify these predictions, experiments have been performed to evaluate the thermoelectric and mechanical performance of the TEDs at various stages of their development. As changes and improvements to the design of the TEDs have been made, the test fixtures and methods to conduct these experiments have undergone changes and improvements as well. Thus, the testing procedures described in the following chapters reflect the changes that have been made through several iterations of tests and improvements.

The first experiments that were conducted tested the performance of a single module. After this, multiples modules were tested under a parallel wiring configuration so that if one module failed, the electrical circuit for the other modules would be uninterrupted. Total power for these tests was estimated to be the sum of the individual power produced by each module. The TEDs consistently demonstrated a module-level thermal efficiency of about 4%. As experiments were conducted that tested 5, 10 and even 20 modules, it became common for at least 1 module to fail during each test. These module failures prompted the suggestion that a method of bypassing failed couples was needed in order to test generators with a series wiring configuration. As a result, significant efforts went into developing the Couple Bypass Technology (see chapter 4).

As a result of the FEA described in the previous section, the cross-sectional area of the TE legs was reduced from 7 mm x 3.5 mm to 3.5 mm x 3.5 mm in order to reduce the amount of thermal stress at the hot side metallization layers. To evaluate the effects of reducing the cross-sectional area, three tests have been conducted since the implementation of the smaller leg size design. The first of these tested a six-couple module, of which one couple was purposefully broken prior to the test. This module was cycled to a hot side temperature of about 685°C. The second tested a single 10-couple module which was cycled to a hot side temperature of about 570°C. The third test cycled two 10-couple modules to 565°C, cooled to room temperature and then cycled again to 700°C. One of the couples in this test was purposefully broken before the test to evaluate the performance of the Couple Bypass Technology. None of the 34 couples that were unbroken prior to these tests broke, even after 19 were cycled a second time in the 2-module test. These results seemed to support the proposal that reducing leg cross-sectional area results in lower stress concentrations at the skutterudite and metallization layer interface.

The success rates of these tests prompted the development of the 100 W test described in this Thesis, using the same fabrication methods and testing procedures of these preliminary tests. The only changes made to the 100 W test were the module insulation type and the brazing agent used to bond the legs to the hot shoe. As only a few modules were being tested, commercial insulation

Fiberfrax Durablanket-S from Unifrax was sufficient to achieve the desired ΔT for these preliminary tests. However, the test described in this Thesis uses the same heat source and contains 20 modules, requiring a more effective insulation to maintain similar ΔT levels. In addition, a brazing agent comparison test conducted before the 100 W test found that couples bonded with a new brazing paste produced slightly more power than couples bonded with the standard brazing foil. Thus, unlike the couples in the preliminary tests, the couples used in the 100 W test were insulated with mica films and aerogel rather than the Durablanket insulation and were bonded using the paste as the brazing agent, rather than the foil.

2.3. Research Questions

Building on the results of these studies and experiments, the 100 W test was designed to answer the following questions:

- Is the current skutterudite thermoelectric generator design able to reliably achieve a power level of 100 W? If not, what roadblocks need to be overcome to consistently achieve this power level?
- Can couple failures be accurately and reliably detected and bypassed to allow thermoelectric generators to be wired in series?

2.4. Summary

A number of previous studies at MSU helped to shape the experiment detailed in this Thesis. A WAVE simulation validated the power goals set for the experiment. A cost analysis established the generator longevity goals and the results of a finite element analysis study prompted a leg size reduction, necessitating changes to the fabrication process described in the next chapter.

Chapter 3

3. Fabrication Process

In order to utilize the thermoelectric properties of materials such as skutterudite, it is beneficial to create individual devices which pair P-type material with N-type material. Manufacturing and testing these individual devices (known as "couples") in a standardized, repeatable manner requires implementation of a fabrication process than minimizes variability. As advancements have been made in TE research, the fabrication process for the TE couples has undergone many changes to incorporate the improvements. The following procedures reflect the current fabrication process used at MSU.

3.1. Materials Synthesis

An essential feature of the TEDs is the TE material itself. Under operating conditions, the ideal TE material has a low value of thermal conductivity and high values of electrical conductivity and thermopower. A figure of merit, ZT, has been established to assess the electrical and thermal properties of a material for use in thermoelectrics:

$$ZT = \frac{S^2\sigma}{\kappa} * T$$

Equation 3-1 Figure of Merit [13]

Where σ is the electrical conductivity, κ is the thermal conductivity, T is the absolute temperature and S is the Seebeck coefficient (or thermopower), which is a measurement of the voltage differential created by a material exposed to a temperature differential, typically expressed in units of microvolts per Kelvin. As a general rule, a thermoelectric couple should have a minimum ZT value of 1 to be considered a feasible material for thermoelectric power generation. Peak values of N-type and P-type skutterudite at 550°C were measured to be approximately 1.15 and 0.85 respectively [14].

While the first traces of skutterudite were discovered naturally, the procedure for synthesizing skutterudite is relatively straight-forward, eliminating the need to procure skutterudite materials from an external source. The procedures detailed in this section describe how the skutterudite is currently synthesized from basic elements at MSU.

3.1.1. Element Mixing

Synthesizing the skutterudite material is a multi-step process which currently takes 4 days to complete. N-type and P-type skutterudites are synthesized in 100-200 gram batches. In order to minimize oxidation, the process is performed almost entirely in either a vacuum or a glove box with an inert atmosphere.

In the first step of this process, the individual elements are weighed on an electronic balance (±0.005 grams) and placed in a tapered glassy carbon crucible. These pure elements are acquired from Alfa Aesar and include Sb ingot (99.9%), Co powder (99.9%), Fe powder (99.999%), Ba pieces (99.9%), Ce pieces (99.9%) and Yb pieces (99.9%) [15]. This crucible is then placed in a 50 mm diameter quartz tube, removed from the glove box and immediately placed on a high vacuum sealing line, which consists of a Varian Turbo Mini Pumping Station (Turbo V70LP) backed by an Edwards RV5 pump. This vacuum sealing line can accommodate quartz tubes ranging from 10 mm to 50 mm in diameter and can reach a vacuum pressure of $1x10^{-6}$ torr. To achieve a pressure of ≈ $4x10^{-6}$ torr, the compound is held under vacuum for about 24 hours before the quartz tube is sealed by placing a slightly smaller diameter quartz plug inside the tube and using a torch to flame seal the tube.

3.1.2. Synthesis and Annealing

On the second day of the process, the sealed quartz tube is removed from the vacuum line and placed in a tube furnace where it is ramped up to 1100°C at a rate of 10°C per minute and held at temperature for about 15 hours. The tube is then air quenched to ensure smaller grain size of the skutterudite precursors. To convert these precursors into a homogeneous skutterudite compound, the mixture is then annealed for 48 hours at 740°C and 700°C for the P-type and N-type skutterudites, respectively.

3.1.3. Powder Processing

The last step is to powder process the skutterudite ingot for hot pressing. After the compound has annealed for 2 days, the quartz tube is moved into the inert atmosphere double glove box and is broken to release the glassy carbon crucible. The ingot is then removed from the crucible and is crushed and ground for five minutes using a motorized mortar and pestle. The powder is then sieved for 30 minutes using a 75 µm test sieve. Any material that doesn't pass through the sieve is reground for 5 minutes and sieved again. This is repeated until approximately 99% of the skutterudite material has passed through the 75 µm test sieve (typically 3 iterations). All the powder is then collected and placed inside a 500 ml stainless steel ball mill jar along with 7 stainless steel balls (20 mm diameter) where it is ball milled for 3 hours at 110 rpm. This reduces the average particle size to approximately 34.9 μm. The skutterudite powder is then removed from the grinding jar and stored in a glass jar until hot pressing.

3.2. Leg Fabrication

While skutterudite has great thermoelectric properties, it fails to form an adequate bond with the copper hot shoes. To address this, metallization layers are added on the top and bottom of the TE legs to provide buffers between the skutterudite material and the hot shoe and cold shoe, respectively. The metallization layers for the P-type legs consist of Material B, followed by Material A and copper foil. The metallization layers for the N-type legs consist of Material A followed by copper foil (Figure 3-1).

Material A forms a good bond with the copper foil, which forms a good bond with both the solder used on the cold side and the brazing agent used on the hot side. As the linear coefficient of thermal expansion (CTE) of Material A is roughly the same as the linear CTE of the N-type skutterudite, no additional metallization layers are necessary. However, the P-type skutterudite has a linear CTE approximately 33% larger than that of Material A, which would result in high levels of shear stress at the skutterudite and Material A interface during operation. Thus, Material B is used as a buffer between the P-type skutterudite and the Material A layer. Material B has a linear CTE roughly the same as P-type skutterudite, but has a greater yield strength by a factor of 6. This enables Material B to better withstand the high levels of shear stress caused by the difference in linear CTE values.

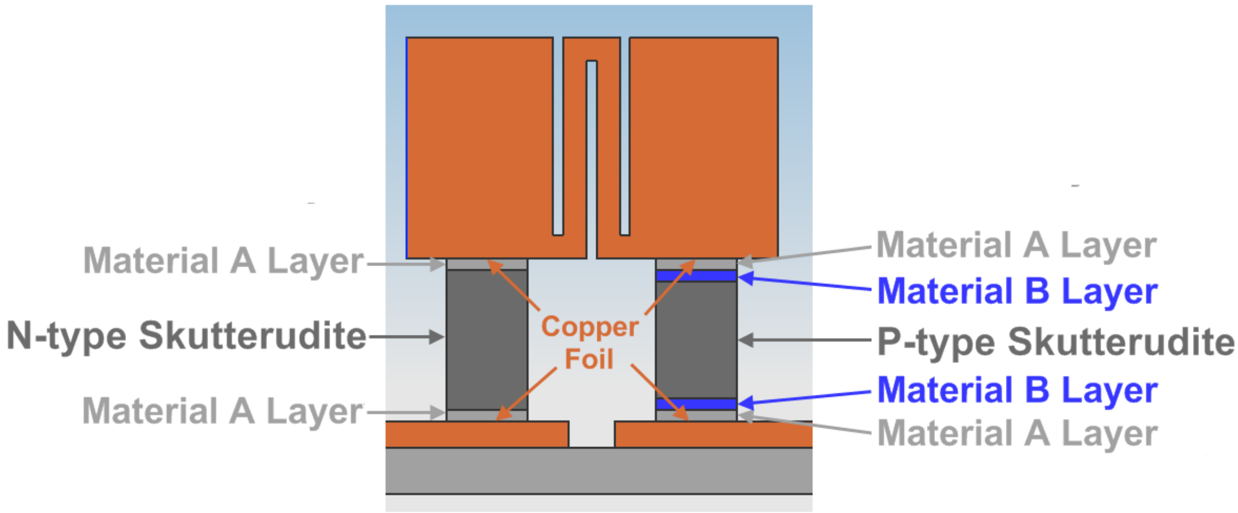

Figure 3-1 Skutterudite Metallization Layers

3.2.1. Hot Press

These metallization layers are sintered with the skutterudite in a Thermal Technology HP200-14020-23G hot press system. This system can achieve a temperature of 2200°C in a vacuum or inert gas and can exert a force of up to 100 tons on a 12 inch diameter by 12 inch high work zone. The temperature and force in the work zone are programmable for simultaneous and independent automatic control. A typical hot press run for a single ingot takes about 6 hours.

To prepare the materials for the hot press, a cylindrical, graphite, powder pressing die is internally lined with Grafoil, a flexible graphite material by GrafTech International. The die has an outer and inner diameter of 6 inches and 2 inches, respectively. After lining with Grafoil, a 2 inch diameter graphite plug is inserted into the bottom of the die such that the bottom of the plug is flush with the bottom of the die. A 2 inch diameter copper foil is then placed inside the die and glued on top of the plug. The assembly is then moved into the double glove box to complete the preparation in an inert atmosphere.

To prepare the N-type skutterudite, Material A powder is first weighed and then placed in the powder pressing die on top of the copper foil. The powder is then cold pressed to 3 tons with a Carver Lab hydraulic press. The die is rotated 90° and cold pressed again. After this, a 2 inch diameter Material C foil is placed on top of the Material A powder. The N-type skutterudite powder is then measured and placed on top of the Material C foil. The powder is cold pressed, rotated and cold pressed again. In the same manner, another layer of Material C foil is placed on top of the skutterudite powder and another layer of Material A powder is placed on top of the Material C foil. After the final cold pressing, a 2 inch diameter graphite plunger is placed on the powder before the die is loaded into the hot press.

To prepare the P-type skutterudite, Material A powder is first weighed and then placed in the powder pressing die on top of the copper foil. The powder is then cold pressed to 3 tons, rotated and pressed again in the same manner as the N-type leg. A 50-50 mixture of Material B powder and P-type skutterudite is added on top of the Material A layer and is cold pressed. A layer of pure P-type skutterudite is added next, followed by another layer of the 50-50 Material B and P-type skutterudite mixture and a final layer of Material A, cold pressing after each layer is added. After the final cold pressing, a 2 inch diameter graphite plunger is placed on the powder before the die is loaded into the hot press.

The die is then loaded into the hot press and the work zone is vacuumed for approximately 1 hour to achieve a pressure of 100 millitorr. After this pressure is reached, the work zone is backfilled with high-purity argon gas (99.999%) to atmospheric pressure and is then vacuumed overnight. To begin the hot press run, the temperature is ramped up to 250°C over 20 minutes to draw out any residual oxygen from the graphite. After this, the work zone is backfilled with argon gas again until a positive pressure of 1 psi is achieved. The argon is then allowed to vent to the atmosphere and a gas flow rate of ≈ 40 liters/hour is maintained for the remainder of the run. Over the next 20 minutes, the temperature is ramped up to 500°C and the hydraulic ram is ramped up to 15,500 kg. After this, the temperature is ramped up to 730°C in 20 minutes under constant force. This is held for 2 hours before the ram is released and the temperature is ramped down to 600°C in 20 minutes. The solid is then allowed to cool to room temperature over 2 hours. The hot press run compresses the material from a height of about 10 mm in powder form to about 7 mm. This solid is called an ingot and is given a unique number for tracking purposes (Figure 3-2).

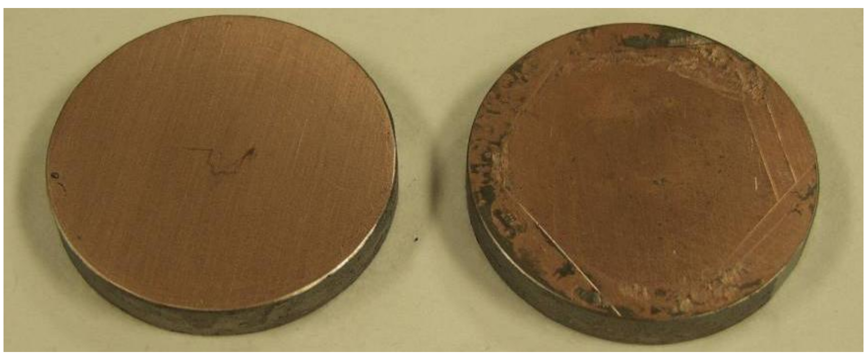

Figure 3-2 Skutterudite Hot-Pressed Ingots

3.2.2. Dicing

After hot pressing, the ingots are diced into legs using a KO Lee grinder/slicer, which is isolated inside a soft wall clean room. The grinder's programmable controller and variable high-speed motor are used to automatically and precisely cut the skutterudite ingots into legs (Y and Z axis ± 0.0001 inch). The diamond cutting blade is 0.017 inches thick and is actively cooled with Omni-cut FC-100 coolant. Figure 3-3 illustrates the cutting diagram for the ingots. It takes about 3 hours to cut both 2 inch diameter ingots into 3.5 mm x 3.5 mm legs.

To prepare the legs for dicing, both ingots are crystal bonded to a graphite-covered steel plate. When the bond sets, the plate is transferred to the KO Lee grinder/slicer, where it is magnetically locked into place. The cutting blade is then adjusted to the correct position and the dicing program is started. After dicing, the steel plate is removed from the grinding machine and placed on a hot pad where it is heated to about 285°C to soften the glue. The legs are then removed from the steel plate and washed in acetone to remove the crystal bond residue. Each N-type and P-type leg pair, designated by matching numbers (see section 3.5.1), is stored in a numbered, glass vial until the bonding process

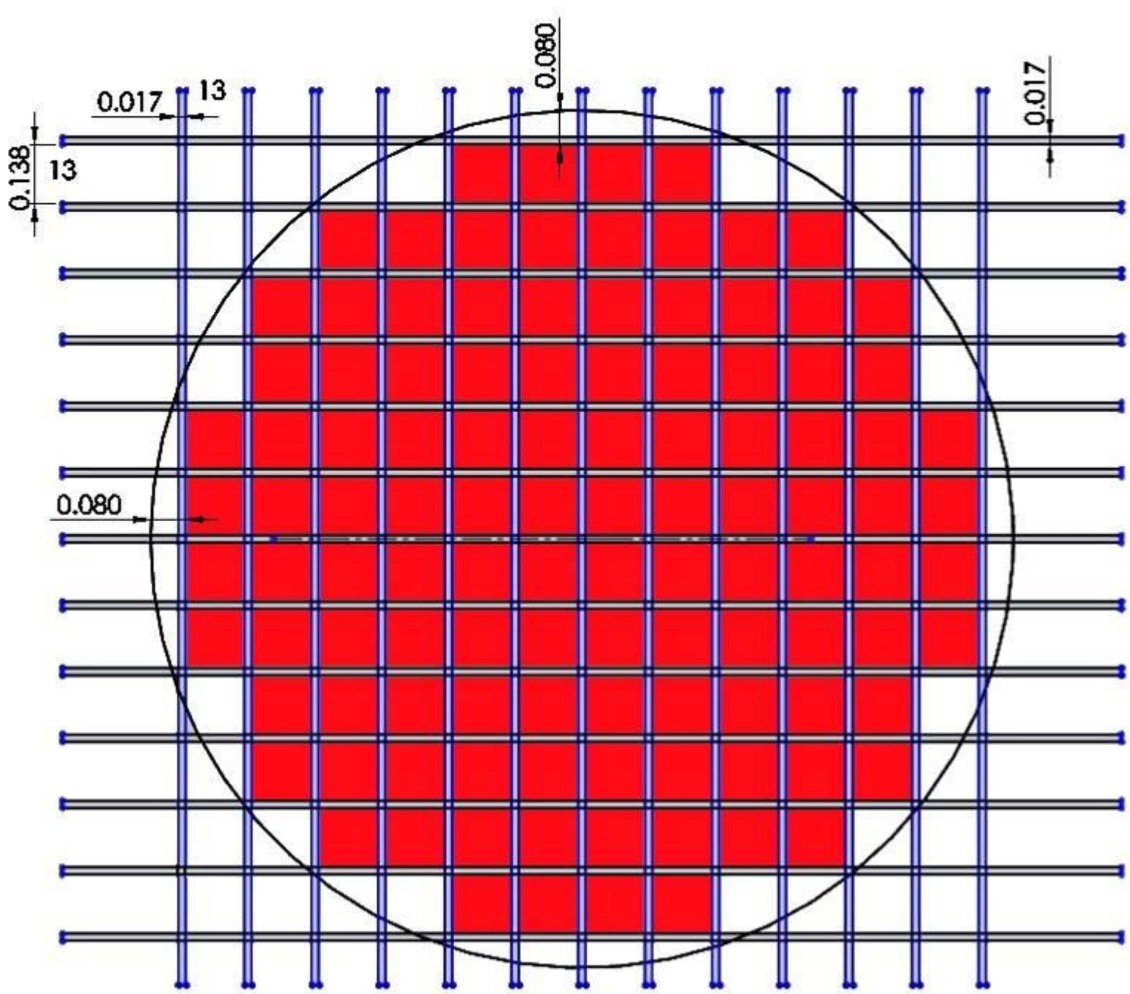

Figure 3-3 Ingot Grinding Diagram

3.3. Couple Assembly

There are several desirable characteristics for a TE couple that have been identified and incorporated into the couples that are currently produced at MSU. An ideal TE couple contains the structural framework to achieve a large temperature gradient while maintaining an electrical circuit that is free from shorts and has high electrical conductivity for maximum power production. A heat collector (commonly referred to as a hot shoe) is used to electrically connect the hot sides of a P-type leg and an N-type leg. The legs should be a standard size and shape to ease fabrication efforts and improve unit modularity. The couple must be physically robust enough to withstand reasonable handling, which is necessary to assemble the couples into modules. These TE couples can be thought of as the building blocks of a thermoelectric generator; greater generator power values must include more TE material, which is accomplished by integrating more couples into the generator design. Figure 3-4 illustrates the current couple design.

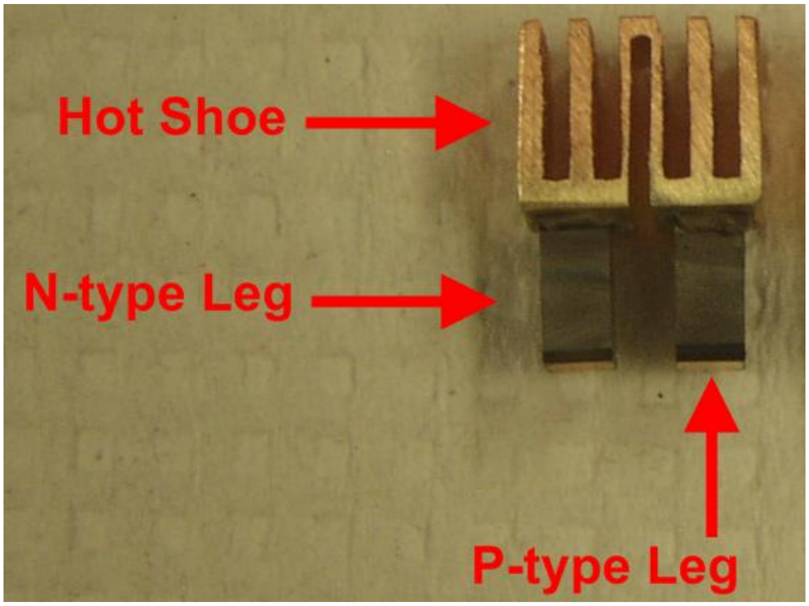

Figure 3-4 Current TE Couple Design

3.3.1. Hot Shoe Design

A vital component of the TE couple is the hot shoe. The ideal hot shoe design maintains a solid bond with the legs, conducts a maximum amount of heat and minimizes electrical resistance between the hot sides of the two legs. Depending on the mode of heat transfer, the hot shoe may also need to allow for differences in thermal expansion between the two legs.

When the primary heat transfer mode is conduction, as is the case with many of the current low-temperature TEG designs, the hot shoe is shaped to maximize heat transfer from the heat source to the legs. It must also be electrically insulated from the heat source to prevent a short circuit. This is the likely hot shoe design for TEGs which must operate in an inert atmosphere.

As convection is the primary mode of heat transfer in the experiment, a new hot shoe design was needed to more effectively transfer heat from the working fluid to the TE legs. A finned design was proposed which increased the surface area of the hot shoe by a factor of 15 for the same cross-sectional area. More importantly, the new design featured an inverted “U” shaped bridge in the middle of the hot shoe which allowed the shoe to flex (Figure 3-4). This flexibility in the hot shoe is important to reduce thermo-mechanical stresses due to different rates of thermal expansion between the P-type and N-type legs. A study by Sakamoto et al. was conducted to estimate the difference in thermal expansion between the legs when heated to a ΔT of 600°C [16]. This difference was compared to the amount of deflection the hot shoe was able to achieve via the inverted “U” shaped bridge. It was concluded that the hot shoe design was more than able to achieve the 10 microns of deflection needed to accommodate the differences in thermal expansion between the N-type and P-type legs at this temperature.

The hot shoes are fabricated using the following method. 1/2 x 3/8 inch copper bar stock is cut and milled into 19/64 inch lengths and deburred. After this, four 0.06 inch wide slots are cut into the copper blocks with a band saw, creating 4 thinner outer fins and 1 thicker middle fin. The hot shoes are deburred again and placed fin-side down in a metal jig. The jig is then placed in the KO Lee grinder/slicer described in section 3.2.2 which grinds a slot down the middle fin. This cut forms the inverted "U" shaped bridge which provides the shoe's flexibility. The hot shoes are then removed from the jig and stored in an acetone bath until the bonding process.

3.3.2. Bonding

The next step in the couple assembly process is to physically bond a skutterudite leg pair to a hot shoe. Currently, the bonding agent used in the fabrication process is Fusion 1000 brazing paste (STL-1000B-658). The skutterudite legs are housed in a graphite jig and aligned with the copper hot shoes with the bonding agent between the leg and hot shoe interfaces. The hot side is heated with a 3 inch diameter oxygen substrate button heater while the cold side is actively cooled with water. The entire bonding procedure is performed in an inert atmosphere inside a Kurt J. Lesker stainless steel vacuum chamber and takes about 2 hours.

The current bonding run procedures begin by selecting 23 leg pairs and sanding both ends of each leg with 400 grit sandpaper to remove oxidation. The legs are then washed in 100% ethanol for at least two minutes and then washed again in fresh ethanol. Meanwhile, 23 copper hot shoes are selected and sanded with 400 grit sandpaper to remove oxidation and any burs incurred by the machining and grinding process. These hot shoes are then etched with tracking numbers corresponding to the numbers of the 23 selected leg pairs, after which the hot shoes are washed in ethanol for at least two minutes and then washed again in fresh ethanol.

A 3 inch diameter graphite jig is used to align the legs with the hot shoes. The jig can accommodate 23 leg pairs at a time and is divided into four sections: the base, the leg mount, the hot shoe mount and the cap. The base supports the leg mount which houses the leg pairs. The leg mount has 2 features that allow the legs to thermally expand with minimal amounts of stress: spring-loaded ceramic rods and spacers made of Grafoil. When properly loaded into the jig, the skutterudite legs rest in paired holes on ceramic rods that are constrained by die compression springs, allowing the legs to expand axially when heated. The Grafoil spacers align the legs away from the inner wall between each hole pair. As the hot side is heated, the copper hot shoe expands laterally until the maximum temperature is reached, melting the paste and bonding the leg to the hot shoe. As the system cools down, the copper hot shoe contracts, pulling the now-bonded legs inward. If the legs are positioned too close to the inner wall before the bonding run, this inward contraction by the hot shoe will cause shear stress at the leg and hot shoe interface, possibly resulting in a break. The Grafoil spacers give the legs room to move with the contracting hot shoe by initially positioning them on the outer edges of the holes.

While the components are being washed in ethanol, forty-six 1/16 x 3/32 inch Grafoil spacers are cut and placed into their respective slots on the leg mount. After the second ethanol bath, the legs are dried and placed into the circular holes such that a P-type leg will be bonded with a same-numbered N-type leg. A bead of brazing paste is then placed on the top surface of each leg via a plastic syringe and the hot shoe mount is placed on the leg mount. The hot shoes are dried and then placed on top of the leg pairs, such that the number etched onto each hot shoe matches the number of the corresponding leg pair. The cap is then placed on top of the hot shoe mount and the entire jig is placed in the bonding apparatus inside the vacuum chamber. This apparatus is designed to heat the top of the jig while actively cooling the bottom. The jig is placed on a water-cooled, spring-loaded copper plate and is insulated with two Fiberfrax Duraboard blocks that are coated with a fireproof sealant. The jig is then secured in place with a 3 inch diameter oxygen substrate button heater which is tightened down two turns after the springs under the cooling plate begin to compress. Two more Duraboard blocks and several Durablanket strips are used to insulate the button heater and the top of the jig. The control thermocouple is then secured in a designated hole in the cap, just above the hot shoes. The lid of the vacuum chamber is then bolted down and the chamber is vacuumed with a BOC Edwards XDS10 dry scroll pump for 5 minutes. The chamber is then backfilled with a 95/5 argon/hydrogen gas mixture to atmospheric pressure and is vacuumed for another 5 minutes. This gas mixture is used in place of high-purity argon gas to reduce the amount of residual oxygen molecules in the chamber by bonding them with hydrogen. The chamber is again backfilled with the gas mixture which maintains a continuous flow of 8 cubic feet per hour (CFH) for the remainder of the bonding run. Once the pressure inside the bonding chamber reaches 2 kPa (gage), the one-way atmosphere valve is opened to allow the gas mixture to vent. The cooling water is then turned on and the bonding run program is initiated.

The button heater is controlled by a programmable Heatwave Labs temperature controller. The bonding run program ramps the temperature up to 700°C in 29 minutes and then dwells for 15 minutes before ramping down to room temperature over 20 minutes. After the system has sufficiently cooled, the jig is removed from the vacuum chamber and the cap and hot shoe mount are removed. If any couples are found to have broken legs after the bonding run, the location of the breakages on the leg and the location of the broken legs in the jig are documented. The non-broken couples are then stored by ingot numbers.

3.3.3. Individual Couple Testing

To assess theoretical power potentials and cycling durability for individual couples and to evaluate the effect that changes in the fabrication process have on power production, a couple testing stand was fabricated. The testing stand is enclosed inside a Kurt J. Lesker Pyrex bell jar station to perform the tests in an inert atmosphere. The couple testing stand is similar to the bonding station; a water-cooled, spring-loaded copper plate actively cools the cold side of the couple while a button heater, controlled by a Heatwave Labs temperature controller raises the hot side temperature to a set value. In the couple testing stand, however, the couple is not placed in a graphite jig. Instead, the hot shoe is in direct contact with the button heater, allowing more precise control over couple hot side temperatures.

To prepare a couple for testing, the couple legs are soldered to separate copper blocks which act as heat sinks and the whole assembly is placed on the copper cooling plate in the bell jar station. Voltage leads and thermocouples are placed such that the voltage difference across each leg is measured along with the hot and cold side temperatures. The control thermocouple is placed in a designated hole in the hot shoe and the couple is insulated with Durablanket. The bell jar is then sealed and the station is purged of oxygen using the same vacuum and backfill method described in the previous section. After backfilling the station with the 95/5 argon/hydrogen gas mixture a second time, the gas flow rate is adjusted to maintain a continuous flow of about 4 CFM throughout the duration of the test. After the test stand reaches a pressure of 0.5 kPa (gage), the one-way atmospheric valve is opened and the testing program is started. The temperature controller ramps the temperature up to 656°C in 30 minutes and then dwells for 15 minutes before ramping down to room temperature over 25 minutes. After the hot side temperature has sufficiently cooled, this cycle is repeated another 8 times.

Eighteen couples of the same and similar material used in the 100 W test were tested using this method.

3.4. Module Assembly

As the power produced by an individual couple is relatively limited (typically around 0.5 to 1 W), it is advantageous to combine several couples into a modular subassembly that electrically connects the couples in series, enhances durability and rigidity, establishes a common cold side heat exchanger and improves ease of generator installation. For example, given an average couple power output of 0.5 W, a 100 W generator would require installing 200 couples. However, if these couples were assembled into 10-couple modules, a 100 W generator would require installing only 20 modules. Thus, the next step in the fabrication process is to assemble the TE couples into 10-couple modules.

3.4.1. Module Board

At the heart of the TE module is the module board. The circuit design of this high-temperature, 2-layer, FR-4 board connects the couples in series and houses 10 electrically activated switches (EASs), ten 0603 resistors and 3 ribbon cable connectors to accommodate the Couple Bypass Technology components described in Chapter 4. As is seen in Figure 3-5, the module board contains 20 holes which align with the legs of 10 couples and 2 holes for 4-40 brass mounting bolts.

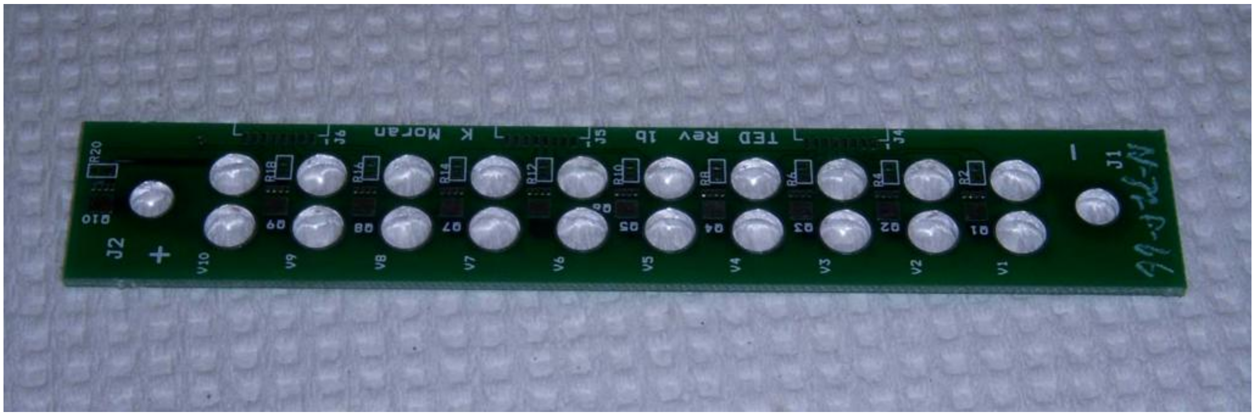

Figure 3-5 Unpopulated Module Board

The first steps in the module assembly process are to solder the ribbon cable connectors to the module board with high-temperature, lead-free solder and the heads of the mounting bolts in their corresponding holes with SnPb 60/40 solder. The board is then etched with a tracking number as well as the ingot numbers of the legs that will be used in the module. Four 0.055 inch diameter through holes are then drilled into the module board, using the clamping bolt holes in the cold plate discussed in section 3.4.3 as a guide. After four 00-90 bolts are inserted though these holes, 00-90 nuts are used to fasten them into place and the bolt heads are secured to the module board with epoxy. After the epoxy has set, the cold plate is removed and the module board is transferred to the soldering station. Figure 3-6 shows the module board at this point.

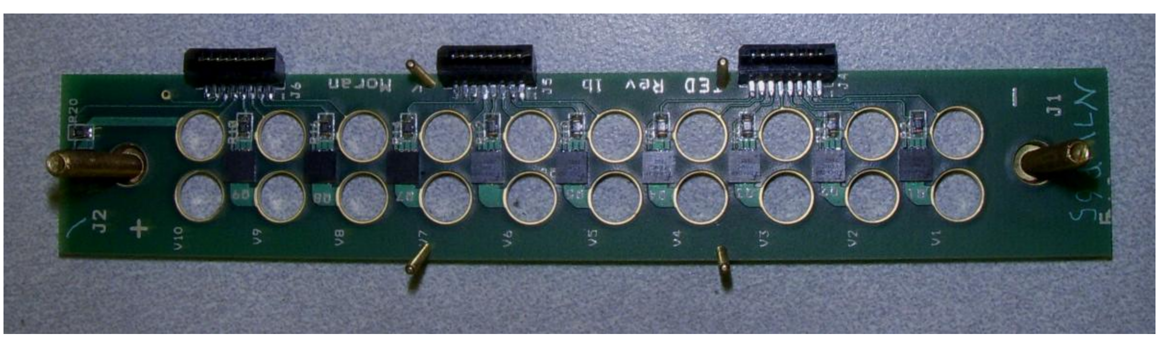

Figure 3-6 Module Board with EASs, Ribbon Cable Connectors, Tracking Number, Mounting Bolts and Clamping Bolts

3.4.2. Insulation

As the power generated by a TED is directly proportional to the ΔT across the skutterudite leg, exceptional insulation of the TE couples is critical to overall generator performance. As such, considerable emphasis has been placed on researching various insulation materials and casting methods. One high performance insulation technology that is receiving serious consideration is titania-opacified aerogel [17]. This silica-based insulation features excellent conductive and convective insulation properties and the added titania effectively scatters infrared radiation. As the aerogel material is very porous and delicate, quartz fibers are added to improve durability. This combination of silica-based aerogel, titania and quartz fibers are referred to in this Thesis simply as "aerogel." While aerogel fabrication methods are beyond the scope of this Thesis, it should be noted that fabrication procedures have been modified from a cast-in-place method to a form-casting method, greatly easing fabrication efforts. In addition to the aerogel forms, 0.875 by 4.5 inch mica films are used to improve module durability and provide additional insulation by overlapping gaps between modules. A finished aerogel form is shown in Figure 3-7.

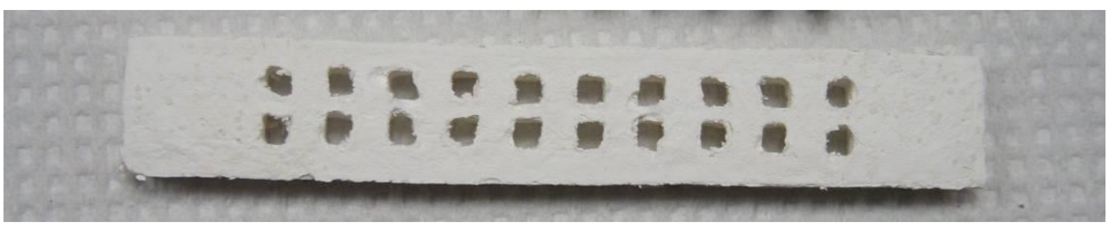

Figure 3-7 Aerogel Form

Once the aerogel forms are ready, 10 TE couples are sanded and placed in the slots in the mica films and aerogel forms. The assembly is then rotated such that the legs protruding through the aerogel are facing upwards. The module board is then placed on top of the aerogel form, aligning the holes with the legs. A soldering iron is used to heat individual pockets, which are filled with SnPb 60/40 solder until flush with the module board. An intermittent pattern is used to more evenly apply the heat and to avoid unintentional de-soldering of existing components. Once all the pockets are filled, flux remover spray is used to clean the solder pads. Heat shrink wrap is then added to the mounting bolts to electrically insulate the cold plate from the bolts. Figure 3-8 and Figure 3-9 show the module at this point. As these pictures were taken after the 100 W test was conducted, significant oxidation of the copper hot shoes can be seen in these figures. The clamping bolts are not shown for Figure 3-9.

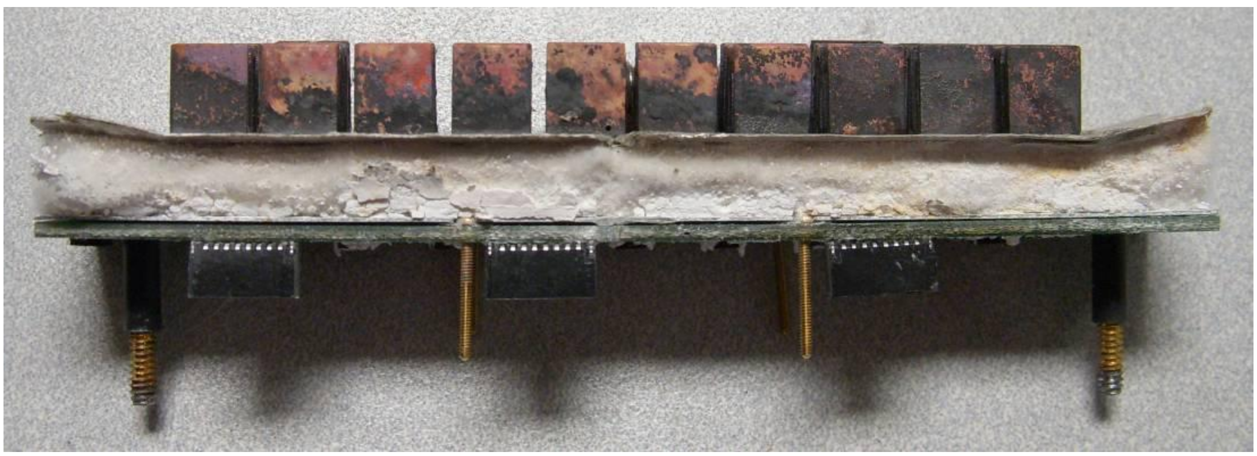

Figure 3-8 Module Board after adding Aerogel Mold, Mica Film and Soldered Couples (Side View)

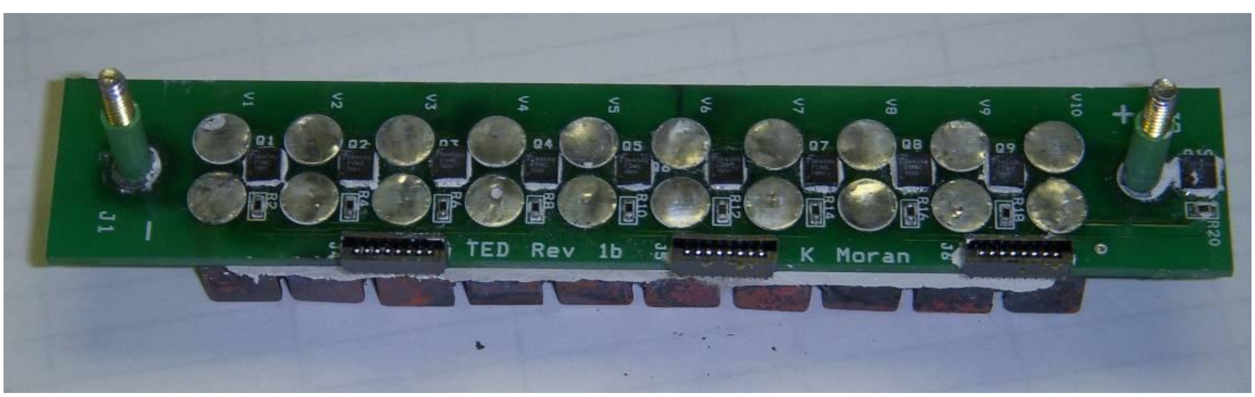

Figure 3-9 Module Board after adding Aerogel Mold, Mica Film and Soldered Couples (Bottom View)

3.4.3. Cold Plate

The function of the cold plate is to direct the cooling fluid as close to the solder pads as possible while providing a physical barrier between the cooling fluid and the electronics on the module board. The cold plate also comprises the frame of the round generator design; each plate is designed to cover 18° of the 5.9 inch diameter of the generator, completing the round shape when all 20 modules are fixed in place.

The cold plates are fabricated using the following process. 3/8 x 1 inch aluminum bar stock is cut and milled into 125 mm lengths. A 9° angle is machined on both sides and ten 1.25 mm pockets are milled on the inner face to accommodate the CBT switches. In addition, ten 0.75 mm pockets are milled on the inner face to accommodate the resistors. Two 5 mm diameter through holes are drilled for the mounting bolts, four 0.055 inch diameter through holes are drilled for the clamping bolts and three 1.5 mm slots are milled for the ribbon cable connectors. Two 1/4 diameter holes are drilled and tapped lengthwise through the plate for the cooling fluid. The cold plates are then anodized at Great Lakes Metal Finishing Inc. to provide electrical insulation from the TEDs.

Once the plates have been anodized, they are etched with a module number and bolted to the module board, aligning the CBT switches with their corresponding slots. The four 0.055 inch diameter through holes in the cold plate are then used to align the holes for the clamping bolts in the module board, as described in section 3.4.1. After the TEGs have been soldered to the module board, the cold plate is coated with a thermal compound (Céramique by Arctic Silver) and is again bolted to the module board, with hard-fiber washers electrically insulating the mounting bolts and nuts from any electrically conductive “hot spot” that may have been exposed during assembly. After the clamping bolts are re-bolted, the module is ready for generator assembly. The final module fabrication steps, which connect the CBT hardware to the module, are completed after the generator is mounted to the Airtorch. Figure 3-10 shows the module at this point. As this picture was taken after the 100 W test, significant oxidation of the copper hot shoes can be seen in this figure.

Figure 3-10 Module with Cold Plate

3.5. Measurements

As TEG fabrication is still in the early stages of development, many cause-and-effect relationships have yet to be determined. To gain a holistic understanding of the diverse factors that affect TEG performance, a tracking system was established and various properties and measurements such as electrical resistivity were recorded. As these cause-and-effect correlations are developed, more intelligent decisions can be made to optimize the fabrication process and TE couple design.

3.5.1. Tracking System

To enable investigation of the relationship between both thermoelectric and mechanical performance and various leg, couple and module properties, a numerical tracking system was established. Properties such as ingot number, location in the ingot, electrical resistivity and bonding run information are recorded and documented for each leg. A number is assigned to each leg, which is also used to pair N-type legs and P-type legs for bonding into TE couples. Figure 3-11 illustrates the leg numbering system with respect to ingot location.

During the bonding process, each skutterudite leg pair is matched with a copper hot shoe etched with the same number. Module boards are etched with the ingot and module numbers and the cold plate is etched with the module number as well. Thus, at any point during fabrication or assembly, it is possible to track the status of an individual leg, from its location in the ingot, to its location in a module to its location in the generator itself. This is crucial for identifying any effect that factors such as material concentrations, hot press conditions, bonding run conditions and electrical resistivity may have on thermoelectric performance.

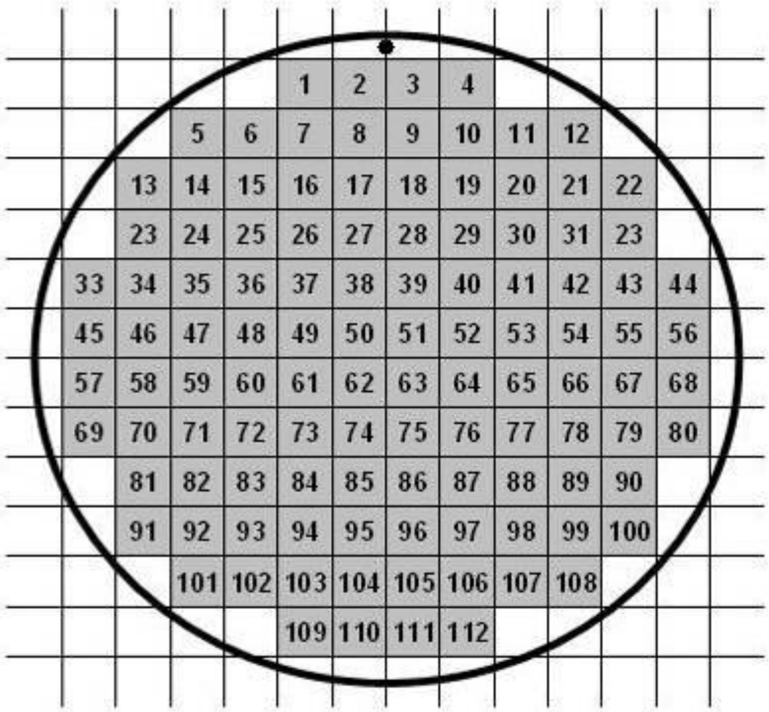

Figure 3-11 TE Couple Tracking Diagram

3.5.2. Electrical Resistivity and Short Circuit

It has been proposed that there is a possible correlation between electrical resistivity and thermoelectric performance. Higher resistance values require higher voltages to achieve the same current, reducing the amount of power a TE couple can produce. Thus, identifying processes or fabrication methods that result in lower resistance values for the couples can result in higher power values for the TEG. To better understand the effect that each step of the fabrication process has on the electrical resistivity of the legs, electrical resistivity measurements are taken after the legs are cut from the ingot, after the legs are bonded to the hot shoes and after the couples have been assembled into modules.

Two separate jigs are used to measure the electrical resistivity of the legs and the couples. The operating method of both of these jigs is the same: two copper leads provide the electrical contact between the legs and a Kepco power supply. One or both of the copper leads is spring-loaded to secure the leg/couple in the jig. The voltage drop across the leg/couple is measured with a multi-meter while applying a current of 1 amp with the power supply. These two values are then used to calculate the electrical resistance of the leg/couple. The electrical resistivity of a module is measured without a jig and instead uses alligator clips attached to the mounting bolts to complete the circuit. Figure 3-12 shows the loaded and unloaded jigs for measuring the electrical resistivity of the TE legs and couples.

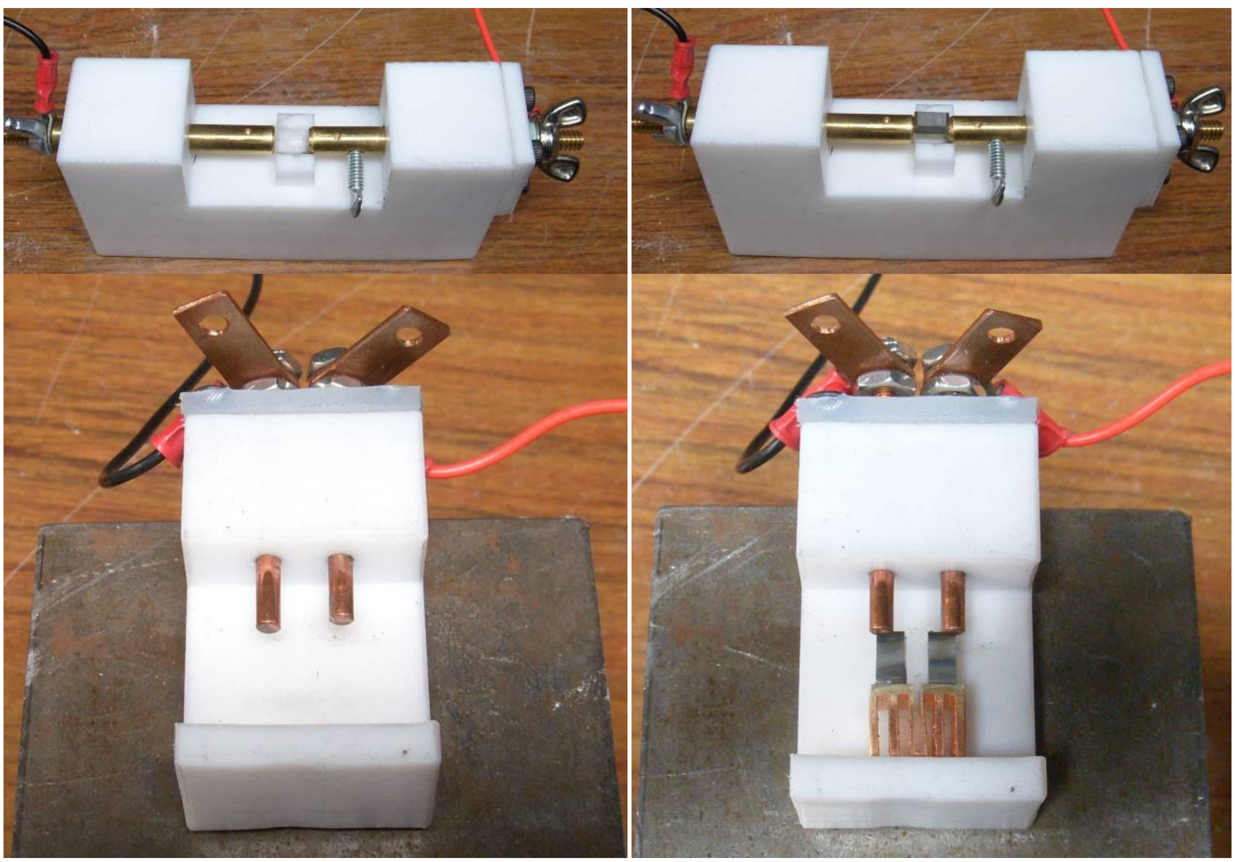

Figure 3-12 Electrical Resistivity Measurement Jigs

After the electrical resistivity measurements, the modules undergo an electrical short circuit test. Because of the high levels of electrical resistivity of the thermoelectric legs compared to the aluminum material that comprises the cold plate, an electrical short circuit would result in almost no power generation, based on voltage divider principles. As such, it is critical to prevent shorts in the circuit connecting the thermoelectric couples. After module fabrication and just before installation in the generator, the modules are all tested for short circuits by placing one lead of a multi-meter on the mounting bolt and the other lead at various locations on module, including the clamping bolts and the surface of the cold plate, and measuring the resistance. If all measurements result in infinite resistance, the module is ready for installation in the generator. Any discovered short circuits are electrically insulated and the module is tested again.

3.6. Summary

The process of fabricating components for the TEG is three-fold. First, pure elements are mixed, placed in a furnace and then annealed to synthesize the skutterudite compounds. This compound is pulverized, layered with film and powdered metals and hot pressed into ingots. These ingots are then cut into TE legs. In the second stage, the legs are arranged into TE couples, consisting of one P-type leg, one N-type leg and a common hot side heat exchanger. These components are bonded together with brazing paste. During the final stage, the couples are arranged into TE modules. Each module houses 10 couples, all wired in series, and provides each with a common cold side heat exchanger. The module also houses the CBT, insulation and cooling infrastructure.

At each stage, electrical resistivity measurements are taken to aid in establishing correlations between both thermoelectric and mechanical performance and leg, couple and module properties. This is facilitated via the established tracking system.

Chapter 4

4. Electronic CBT

The power produced by thermoelectric devices is directly proportional to the temperature difference between the hot side and the cold side of the thermoelectric legs. In order to achieve the desired power output of 0.5 W per couple, a considerable temperature difference of about 475°C is required. This results in a significant temperature gradient of over 1700°C per inch. These extreme conditions in which the thermoelectric couples must operate pose a considerable risk to the integrity of the thermoelectric legs. As the couples are wired in series, this risk jeopardizes the overall power of the generator; if just one couple in a 10-couple module fails structurally, it breaks the electric circuit for the other nine couples, effectively negating their contribution to the overall power. Higher voltages require multiple modules to be wired in series, multiplying the power loss caused by a broken couple. To address this risk, the Couple Bypass Technology (CBT) was developed.

4.1. Overview

The CBT is an electronic solution that incorporates the use of electrically activated switches (EASs) to protect against couple failures. When a particular EAS is closed, it establishes a low-resistance path in parallel with the corresponding thermoelectric couple. This is useful when a couple degrades to the point where it is no longer contributing power to the circuit, but is acting more like a load due to an increase in internal resistance that accompanies couple degradation. More importantly, the low-resistance path established by a closed EAS enables the generator circuit to bypass a couple that has failed to the point that it acts as an open circuit, allowing utilization of the power produced by the other non-broken couples in the series circuit. However, experiments have shown that about 0.5 W -the amount of power each couple is predicted to produce during operation- is absorbed by a closed EAS. This power must be supplied by the other couples in the series; if one couple fails, the power produced by another couple is absorbed by the closed EAS while bypassing the failed couple. Thus, while the EASs provide a way to bypass degrading or failed couples, they place an additional load on the circuit in the process. Because of this, CBT for future generators should not be viewed as a way to accommodate fragile TE material or sloppy fabrication and installation procedures, but rather as a short-term solution to maintain a closed circuit and minimize power losses in the TEG until adequate repairs can be made.

As skutterudite research is still in the early stages, design improvements such as material robustness and bond durability are ongoing, compelling present generator testing research to be completed with the present TE couple design, which is known to have integrity liabilities at the hot side interface. To account for these liabilities, the present CBT design monitors the status of every couple during generator testing and is able to bypass any individual couple that either has degraded to the point of acting as a load on the circuit, or has physically fractured such that it acts as an open circuit. Both of these failures compromise total power production, which is the primary goal for the 100 W test. Thus, for the present generator testing research, the CBT is designed to bypass any failed couple as needed to minimize power losses. As skutterudite materials technology becomes more advanced, such that couple breakages during operation are rare, this design can be simplified to monitor and short entire modules, rather than individual couples, reducing the complexity and power requirements of the CBT.

4.2. Design

The primary objective of the CBT is to provide the capability to bypass any TE couple that fails during the 100 W test. In order to short any couple, one EAS is wired in parallel with each couple and is closed only when a failure is present (Figure 4-1). To detect a couple failure, measurements are taken across every couple to obtain the voltage differential. In addition, the voltage change across each module is measured directly using a voltage divider.

When a couple slowly degrades during operation, the internal resistance of the TE legs gradually increases. Once the couple has degraded to the point that the measured voltage differential across the couple falls below a specified threshold for a certain amount of time, the corresponding EAS is closed, allowing the current to flow through the EAS, which has lower resistance than the failing couple. While this bypassing reduces the voltage drop across the couple, the voltage change across the EAS is still negative and is on the order of 20-60 mV, resulting from the following relation:

$$V_{EAS} = -I * R_{EAS}$$

Equation 4-1 Voltage Load for Failed couple [18]

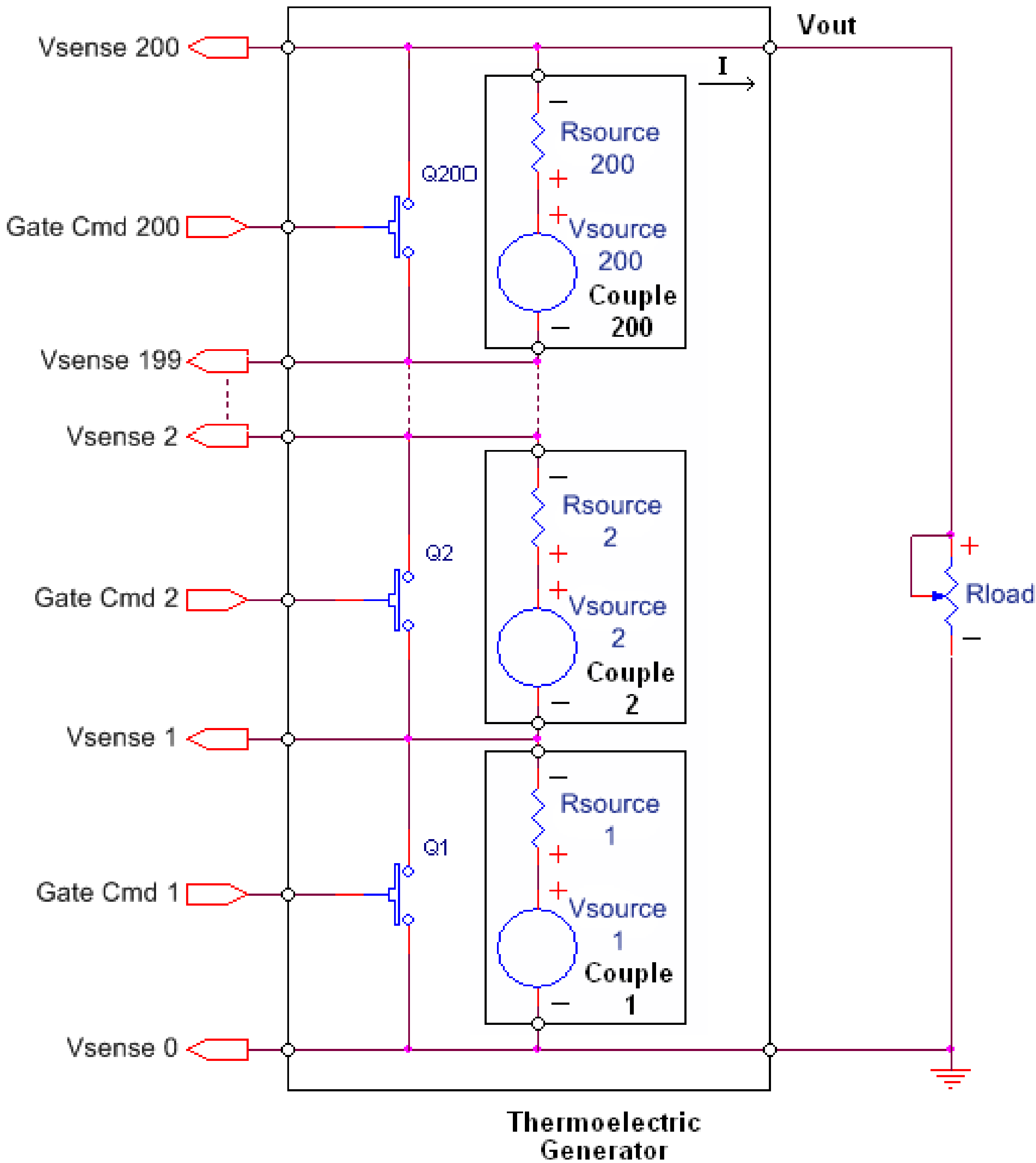

Figure 4-1 EAS Placement Schematic [19]

4.2.1. Hardware

The present CBT design features 2 circuit boards: the module board and the microprocessor board. The module board (described in section 3.4.1) houses the EASs as well as 3 ribbon cable connectors for communicating with the microprocessor board. The microprocessor board is populated with a Freescale MC9S08DZ60 microcontroller and supporting circuitry, including 3 ribbon cable connectors to enable communication with the module board. Depending on the testing objectives, this microprocessor board can be programmed to control the EASs independently and automatically, or with a supervisory controller. Communication with the optional supervisory controller and data acquisition system is achieved via a CAN (Controller Area Network) transceiver. Future CBT designs that utilize module-level, rather the couple-level bypassing methods will feature simplified circuitry and reduced power requirements, enhancing the feasibility of powering the microprocessor board internally. Figure 4-2 displays the top view of the microprocessor board.

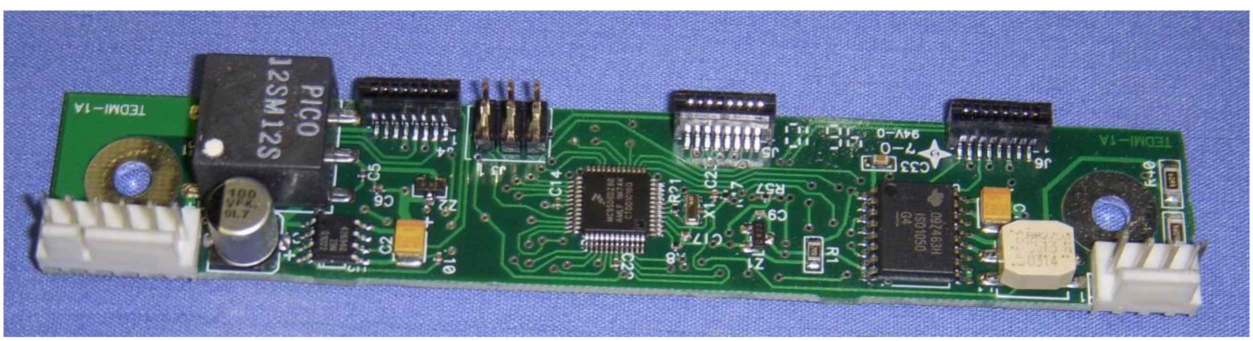

Figure 4-2 Microprocessor Board

A significant hardware consideration that needed to be addressed when designing the CBT was how to supply sufficient EAS activation-signal-to-low-side voltage for each of the 200 series-connected EASs. The resistance across the EAS, denoted R_{EAS}, is a function of the difference between the activation signal voltage and the low side voltage, which are indicated in Figure 4-3. Larger values of this voltage difference, denoted V_{AL}, correspond to smaller values of R_{EAS} and thus, a smaller voltage drop across the EAS. Ideally, this voltage difference should be around 8-12 V to minimize R_{EAS} and the power absorbed by a closed EAS.

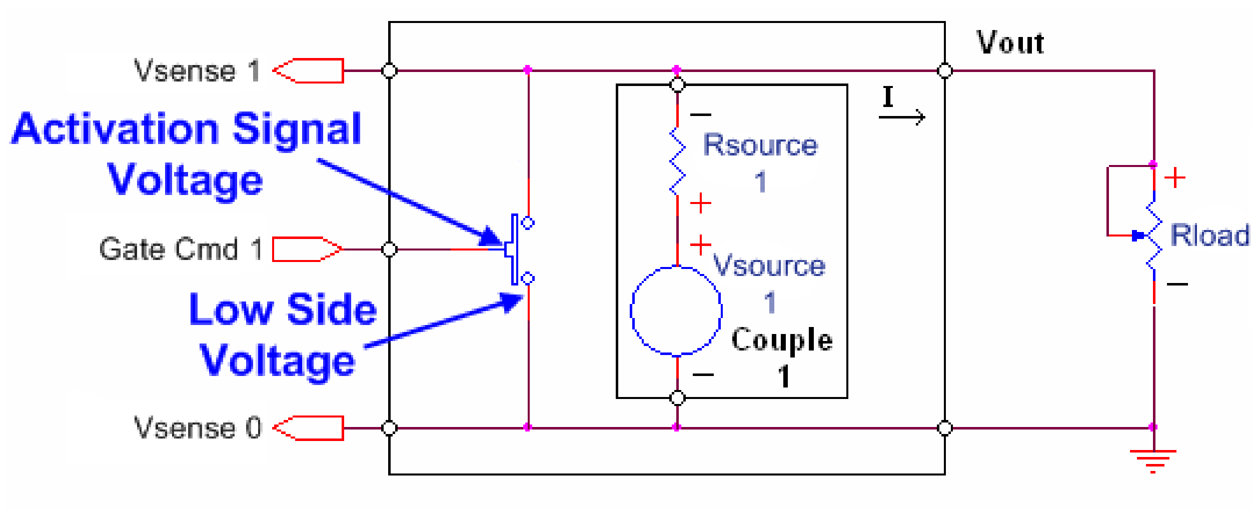

Figure 4-3 EAS Activation Signal and Low Side Voltages

If a couple is functioning normally and the corresponding EAS is open, the V_{AL} term is insignificant since no current is passing through the EAS. The 12 V power supply for the microprocessor board supplies the activation signal voltage for a closed EAS. Thus, the activation signal voltage for a closed EAS is 12 V. However, as the couples and modules are wired in series, the low side voltage increases after each non-broken couple. This is illustrated in Figure 4-4.

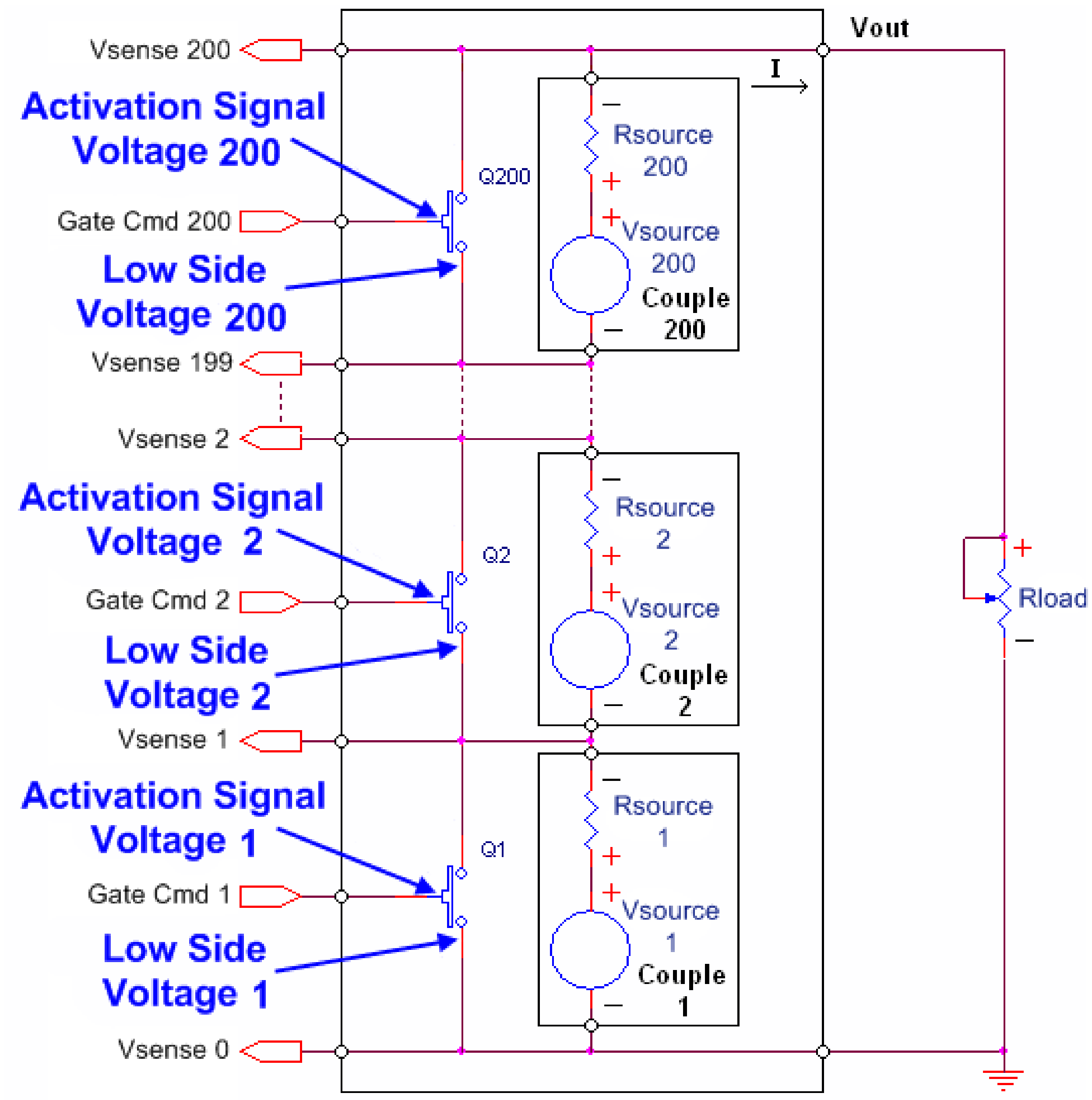

Figure 4-4 Additive Principle of Low Side Voltages

As the low side voltage for the first couple in Figure 4-4 is tied to ground and is therefore zero, the value of V_{AL} for the first EAS is simply the activation signal voltage, 12 V. Assuming that couple 1 is non-broken and thus producing power, the low side voltage for the second couple is the value of low side voltage 1, *plus* the voltage produced by couple 1. Thus, the value of V_{AL}

for the second EAS is 12 V *minus* the voltage produced by couple 1. Following the same logic and assumptions, the value of low side voltage 200 is the sum of the voltages produced by all of the previous couples. This reduces the value of V_{AL} for EAS 200 to 12 V minus the voltage produced by couples 1 through 199. This increasing low side voltage steadily decreases the value of V_{AL} which raises the value of R_{EAS} and thus, the voltage drop across the EAS. As each couple is expected to produce an open-circuit voltage of about 0.15 V, this adding of low side voltages is significant, reducing the value of VAL to zero by the 80th couple.

To account for this incrementally increasing value of low side voltage, a floating power supply was installed in each microprocessor board to establish a local floating ground. The floating power supply uses a DC-DC convertor to provide a 12 V supply to the microprocessor board with a floating ground tied to the positive terminal (or output voltage) of the previous module. For example, if the first module in the generator produces 1.5 V, the value of the local ground for the second module is 1.5 V, relative to the system ground. Additionally, the power supply is offset by 1.5 V, relative to the system ground. Thus, while the local voltage values of power supply and ground for the microprocessor board are 12 V and 0 V respectively, the voltage values relative to the system ground are 13.5 V and 1.5 V, respectively. So while the absolute ground and supply voltages are different for each microprocessor board in the generator, they all maintain a voltage difference of 12 V. More importantly, by offsetting the ground and supply voltages by the positive terminal voltage of the previous module, the floating power supply effectively "resets" the low side voltage of the first couple in each module back to a local value of 0 V, regardless of the increase of low side voltage in the previous module. This sets the VAL value of the first EAS in each module back to 12 V **(Figure 4-5).**

While the increase in low side voltage across each module is thus isolated from the subsequent modules in the generator, the voltage gain across each functioning couple increases the low side voltage for the subsequent couples within that module. However, as the voltage produced by each couple is limited, the total increase in low side voltage within a single module is not significant. Assuming that each couple in a module produces 0.15 V, the first EAS in a module would have a VAL value of 12 V and the last EAS would have a VAL value of 10.65 V. These both fall within our ideal range, resulting in low values of REAS and thus, a minimal voltage drop across the EAS. Minimizing the voltage drop across the EASs is critical as the very purpose of the CBT is to facilitate maximum power production from the TE couples by minimizing power losses

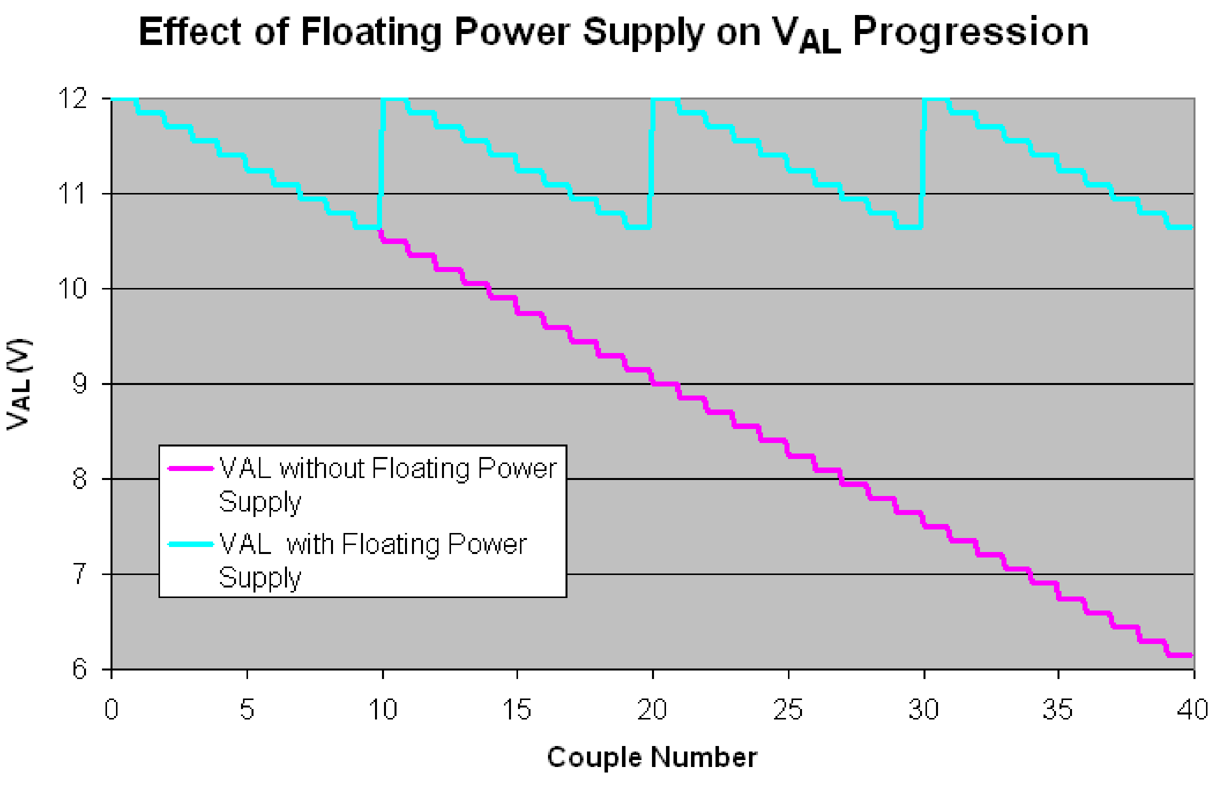

Figure 4-5 Benefits of Floating Power Supply

4.2.2. Software

The task of designing and coding the programming logic to enable the microcontrollers to monitor the differential voltages across the couples and control the EAS activation was outsourced by MSU. After the code was written in C and compiled, PE Micro hardware and software was used to flash the code onto the microprocessor board at MSU.

Under the current program, the microprocessor boards power up in the default mode of automatic control and actively monitor the differential voltages across each couple, the OPEN/CLOSED status of each EAS and the overall voltage change across the entire module. If the differential voltage of any couple drops below the default threshold value, a counter is started. If the voltage remains below the threshold value until the counter reaches the default delay count, the microcontroller closes the corresponding EAS. Once an EAS has been activated, it will not reset until the module is powered down, or is manually instructed to reset by the supervisory controller.

4.2.3. Data Acquisition and Supervisory Control

For current testing purposes, additional coding is included in the software for data acquisition and optional, manual control of EAS activation. This communication is achieved via a dSpace AutoBox and the CAN. The present configuration of the data acquisition program incrementally requests information from the microcontrollers, cycling through all 20 modules every 500 milliseconds. The information collected and displayed for real-time observation during testing includes the differential voltages across each couple, the OPEN/CLOSED status of each EAS and the overall voltage change across the entire module. Because all of this information is transferred through a single CAN Bus, the requests are addressed to identify which module is transmitting the information.

The external controller can also send addressed commands to the microcontrollers to manually open or close specific EASs as needed for testing purposes. There are three commands available to the external controller: close EAS and remain in manual mode, open EAS and remain in manual mode and open EAS and switch to automatic mode. When an EAS is in manual mode, it will not change its open/closed status until it is powered down, unless instructed to do so by the supervisory controller. When the EAS receives a command from the supervisory controller to open and switch to automatic mode, the microcontroller again begins monitoring the voltage differential across the corresponding couple and will automatically close the EAS if the voltage again drops below the threshold for a specified amount of time. Figure 4-6 shows the schematic for the entire CBT system.

In order to sustain sufficiently high values of V_{AL}, each of the microprocessor boards has a floating power supply which ties the floating ground to the positive terminal of the previous module (see section 4.2.1). Because of the difference in local ground values relative to the system ground, each of the microprocessor boards contains an isolated CAN transceiver to enable communication with the supervisory controller.

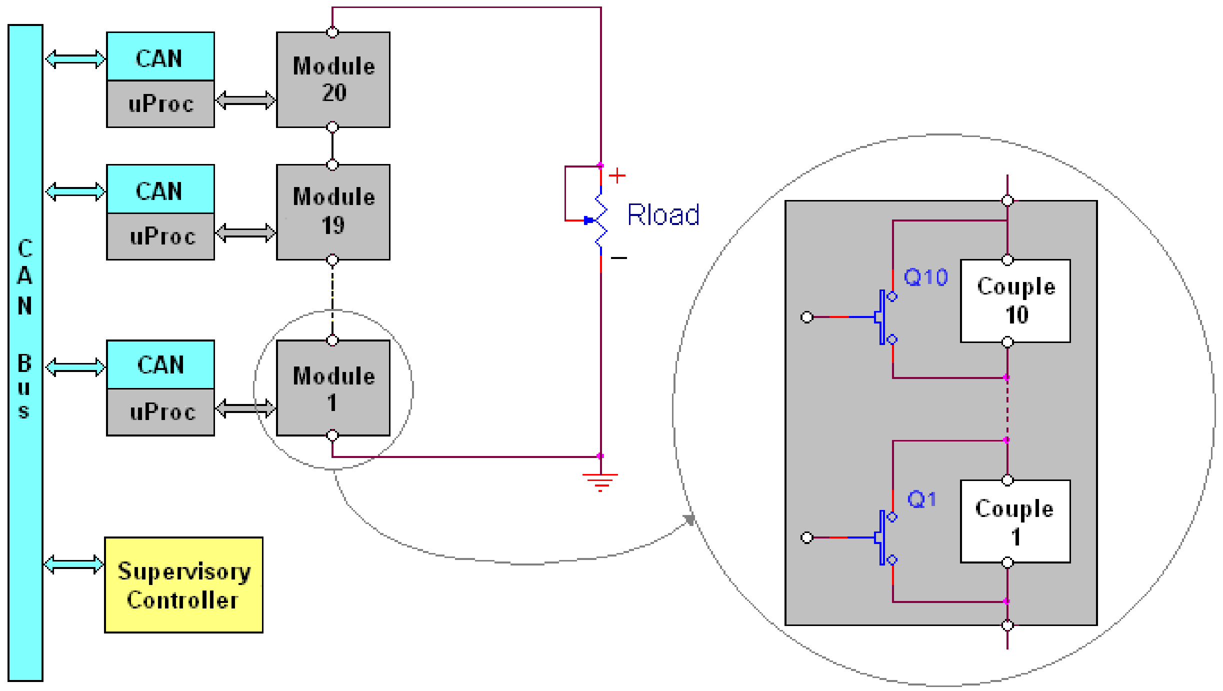

Figure 4-6 CBT Schematic [20]

4.3. Fabrication

The module board fabrication is currently outsourced to Hughes Electronics where the EASs and resistors are added to the high temperature FR-4 circuit board. The ribbon cable connecters are added at MSU before the board is populated with the TE couples and mounted to the cold plates (see section 3.4.1). The 4-layer, FR-4 microprocessor boards are currently fabricated at Semiconductor Hybrid Assembly Inc. where they are populated with the microcontrollers, isolated CAN transceivers, ribbon cable connectors and supporting circuitry and hardware. The microcontrollers are flashed at MSU before the microprocessor boards are installed onto the modules.

The final assembly step for module fabrication is to install the microprocessor board onto the module. This is completed after the generator is mounted to the Airtorch to prevent damage to the microprocessor boards and accompanying ribbon cables (see section 5.1.2). After the generator has been secured, a second nut is added to each mounting bolt. This is to provide adequate spacing for the microprocessor boards, which are oriented such that the ribbon cable connectors on the microprocessor boards align laterally with the ribbon cable connectors on the module boards. The microprocessor boards are then bolted to the outside of the module using a third nut to secure the boards to the mounting bolts. Three Parlex Corporation 8-channel ribbon cables are then inserted into the ribbon cable connectors of each module board and the corresponding microprocessor board. Figure 4-7 illustrates this installation process with a single module.

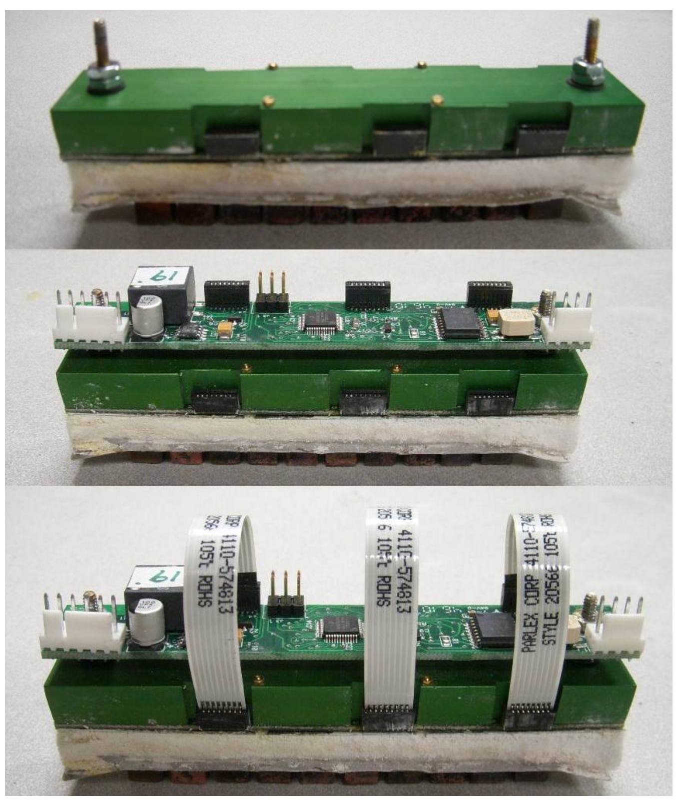

Figure 4-7 Installation of the Microprocessor Board and Ribbon Cable onto Module

4.4. Summary

To achieve the high voltages levels required for commercial feasibility, it is necessary to wire many TE couples in series. This configuration places the power production of the entire circuit at risk in the event of a failed couple. The Couple Bypass Technology is an electronic solution that incorporates the use of electrically activated switches to provide a low-resistance path in parallel with any couples that fail during operation. This not only protects against open circuit failures, but also power losses that occur from extensive couple degradation. The CBT allows higher voltage generators to be constructed without the risk of a failed couple compromising the power production of the entire generator.

Chapter 5

5. Testing

As stated earlier, the focus of this Thesis is to apply the knowledge gained from theoretical thermoelectric research to an experiment simulating real-world conditions. Experiments tend to reveal characteristics of the specimens being tested that are not predicted by theoretical research. As such, it is expected that several iterations of testing, analyzing and quantifying the results, adjusting the testing parameters as needed and then testing again will be necessary to fully understand and control the behavior and performance of these TEDs. This large-scale, multiple-unit testing described here represents the first of its kind with skutterudite thermoelectrics.

5.1. Generator Design

The area of application in question for TEG implementation is the exhaust system of OTR trucks. The potential waste heat recovery opportunity lies in transferring the heat in the exhaust flow to the TE legs, via the hot shoe heat collectors. One of the most effective modes of transferring heat from a fluid to a surface is jet impingement. However, while jet impingement features superior heat transfer characteristics, it also brings several components of the current TEG design that are subject to oxidation at the high operating temperatures into direct contact with the working fluid. This direct contact renders the current TEG design unsuitable for jet impingement with flows containing oxygen, such as Diesel exhaust. However, the tremendous heat transfer benefits associated with jet impingement merit further investigation of ways to integrate skutterudite TE technology in oxygen-rich flows without causing oxidation.

Consequently, the current generator design uses a flow divider to channel fluid streams onto each of the hot shoes, enabling investigation of the effects of using jet impingement as the method of heat transfer.

5.1.1. Module Housing

The round TEG design is made up of 2 endplates and the 20 modules themselves. The 2 endplates are 6.5 inch diameter aluminum rings with 40 tapped through holes for coolant access, 4 tapped through holes for mounting and 2 coolant ports. The endplates feature an internal channel that connects all 40 through holes with the 2 coolant ports. The two 9° angles cut into each cold plate enable the modules to be assembled in a circle, with the hot shoes facing the center (Figure 5-1). The modules are bolted to the endplates, using o-rings to ensure a water-tight seal. The mica films are staggered such that they overlap one another to mitigate air leaks between the modules. After both endplates have been secured, Durablanket insulation strips are placed at both ends to further prevent heat loss. This unit is referred to as a generator and is fully assembled after it is secured to the Airtorch and final components have been installed (Figure 5-2).

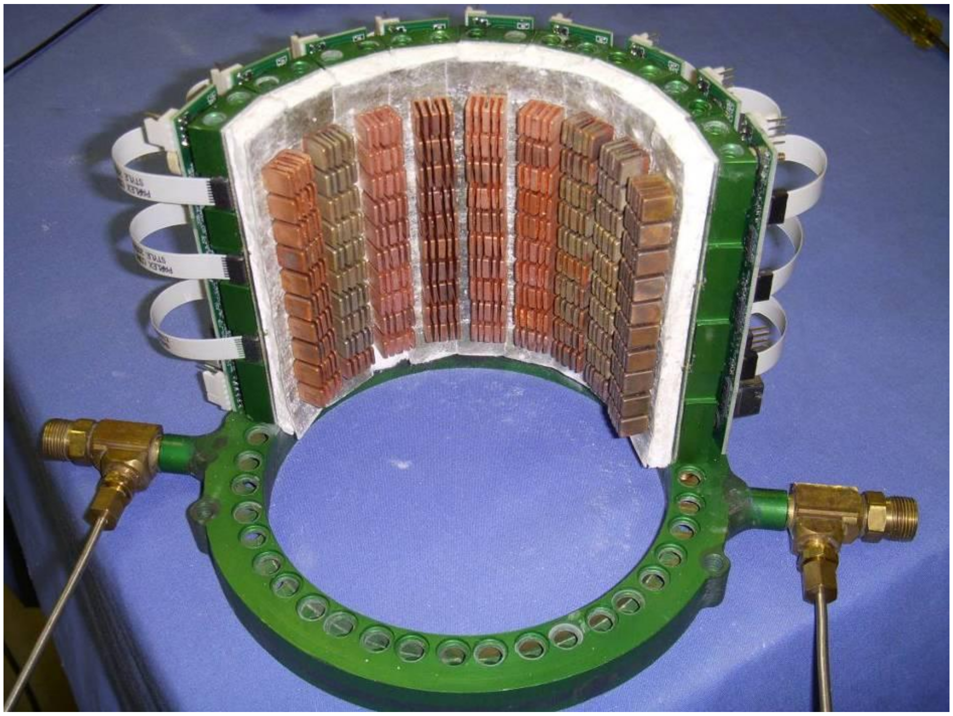

Figure 5-1 Partially Assembled TEG

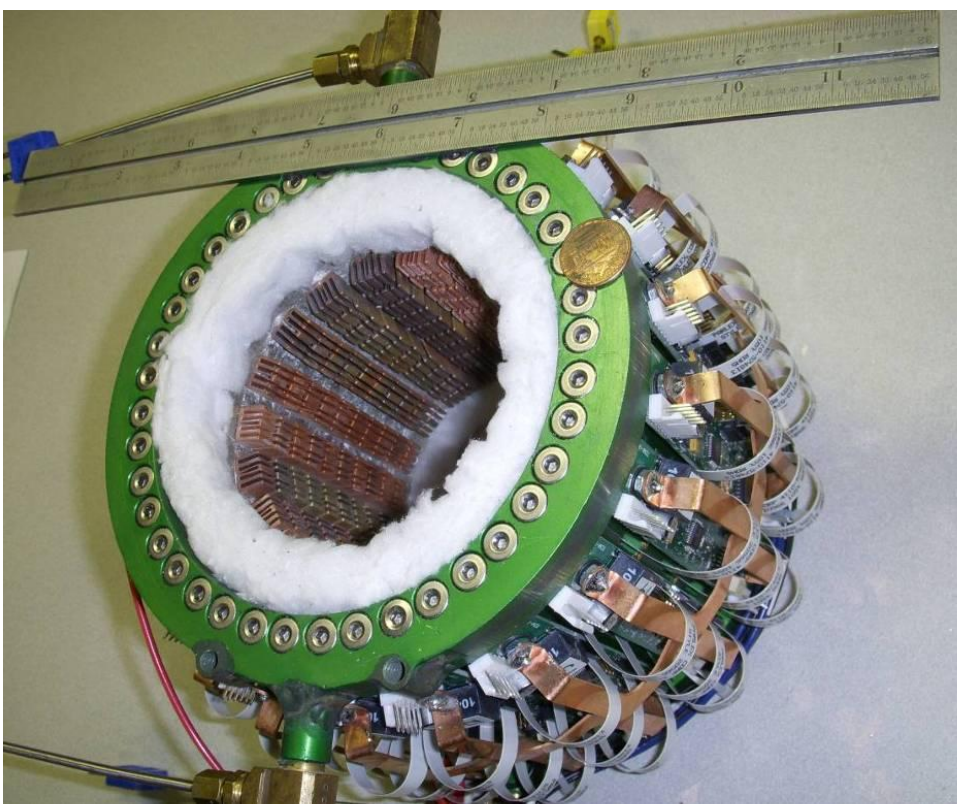

Figure 5-2 TEG with CBT Hardware

5.1.2. Heat Source

To derive logical values for heat source flow rate and temperature, corresponding values from a Cummins ISX engine [21] were used. These conditions were simulated with a 12 kW MHI Airtorch (MTA925-12) and controller. The Airtorch is capable of achieving temperatures of 925°C with an air flow rate of 14.4 cubic feet per minute (CFM). A steel, cylindrical air diffuser featuring 20 rows of five 0.785 inch diameter holes was bolted to the outlet of the Airtorch to provide the jet impingement. A mica gasket was placed between the air diffuser and the Airtorch to seal the interface. The TEG was then bolted concentrically to the Airtorch around the air diffuser such that none of the hot shoes came in contact with the air diffuser (Figure 5-3). A high-alumina ceramic gasket was placed between the air diffuser and the generator to seal the interface. A stainless steel nozzle was then bolted to the outlet of the generator, using a mica gasket to seal the interface (Figure 5-4). The nozzle features a vented exhauster which connects to a building exhaust hose. The vents prevent a pressure drop inside the generator when the building exhaust hose is pumping at a greater rate than the gas is being supplied. The Airtorch and the nozzle were insulated with Durablanket to minimize heat loss to the surroundings.

As mentioned in section 5.1, the current TEG design exposes several components that are subject to oxidation at higher temperatures to the working fluid. In OTR truck applications, this working fluid is oxygen-containing Diesel exhaust. As the purpose of this experiment is not to test methods of insulating the oxygen-sensitive components from the flow, but rather to test the performance of the TEDs under temperature and flow conditions similar to those in the exhaust system of an OTR truck, nitrogen gas was used as the working fluid. This allowed the test to be performed with environmental conditions similar to air, but without the oxidation effect.

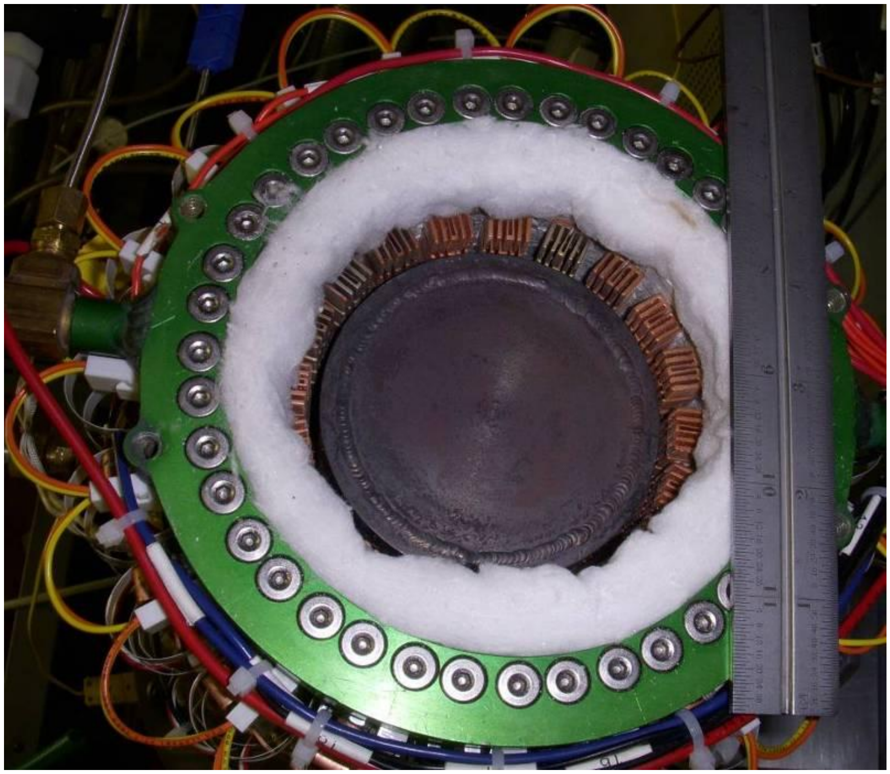

Figure 5-3 TEG with Air Diffuser

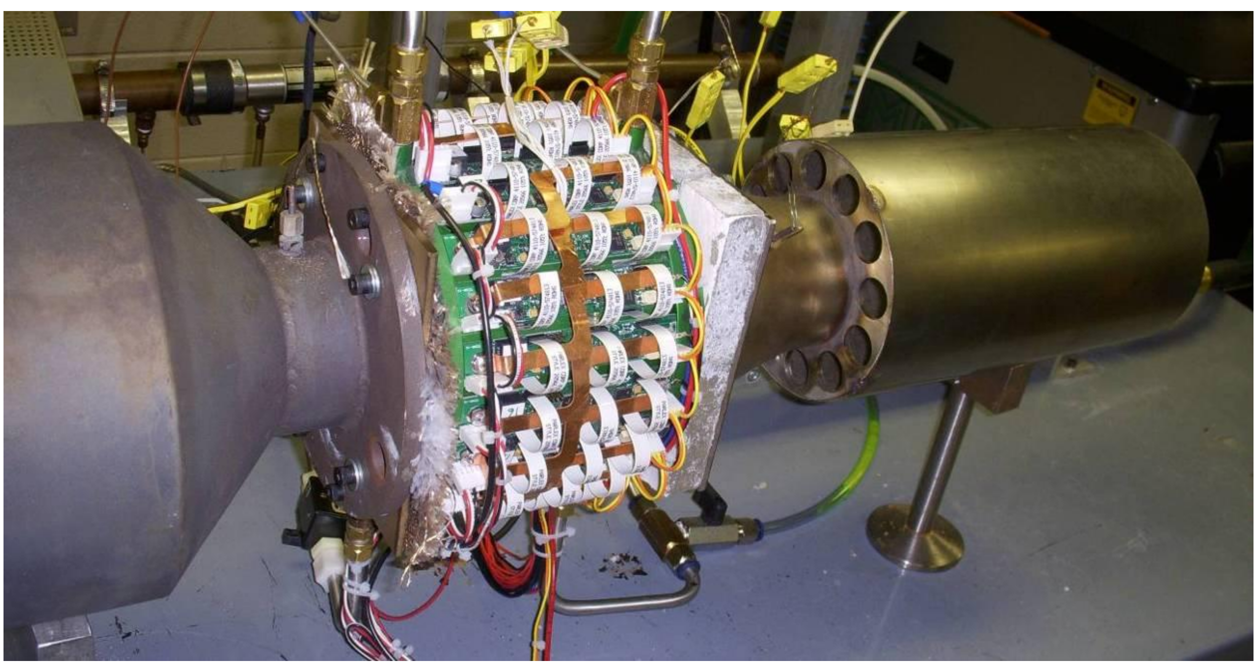

Figure 5-4 Fully Assembled TEG Mounted to Airtorch and Exhauster

5.1.3. Cooling System

The endplates described in section 5.1.1 function as the coolant distributer and receiver for the generator. After the coolant supply lines are attached to the coolant ports of the upstream endplate, cooling fluid is able to access the entire endplate via the channel that connects all 40 through holes.

The bolts used to fasten the modules to the endplates are banjo bolts which feature a lateral through hole in the threads which intersects with an axial hole through the shaft. This allows fluid in the endplate channel to enter the shaft of the bolt laterally and exit axially, which is exactly how the coolant accesses the 2 lengthwise through holes in each cold plate. The coolant exits the cold plate into the downstream endplate in the same manner. Attaching the coolant return lines to the coolant ports of the downstream endplate completes the coolant loop.

To test the TEDs over a greater ΔT range, a 5-ton Temptek CF series chiller was used to create a closed-loop cooling cycle with a 50/50 propylene glycol-water mixture as the coolant.

5.1.4. Instrumentation & Data Acquisition System

After the generator is secured to the Airtorch, the microprocessor boards and ribbon cables are installed as described in section 4.3. Nineteen staggered copper strips are then soldered on to the mounting bolts of sequential modules to connect all 20 modules in series. At this point, the generator hardware is completely installed.

To enable heat transfer analysis and to gain a greater understanding of the forces at work inside the generator during operation, a data acquisition system was implemented. Omega OMB-DAQ-

56 Data Acquisition Modules and the accompanying Personal Daqview software system were used for the data acquisition. Measurements of all properties were recorded every three seconds during the test. All temperatures were measured using Omega K-type and T-type standard thermocouples. Module voltages were measured with 22 AWG wire soldered to the mounting bolts of each module. Organized by system, the following properties were measured:

Pre-heater

- Nitrogen temperature (K-type thermocouple)
- Nitrogen flow rate, measured using a Meriam 50MH10 laminar flow element

Heater

- Nitrogen temperature after Airtorch heater (K-type), grid of 2

TEG

- TED hot shoe temperature (K-type), located on couple 6 in module 20
- TED cold side temperature (K-type), located in the module board below couple 6 in module 20
- Stream wall temperature (K-type), located next to couple 6 in module 20
- Module voltage

Exhaust

- Nitrogen temperature (K-type), grid of 5

Coolant

- Coolant flow rate, measured using two Omega FLR 1000 flow sensors
- Inlet coolant temperature (T-type)
- Outlet coolant temperature (T-type)

During the test, the power produced by the generator is obtained by measuring the generator voltage at different currents. A Kepco power supply is used to back load the generator at specified current levels. The current is incremented and the voltage for each current is documented to find the maximum power according to the common relation: $P = VI$. The theoretical voltage at which maximum power occurs can be calculated using the following equation:

$$P_{Max} = \frac{V_{O.C.}}{2}$$

Equation 5-1 Maximum Power Calculation Equation

Where P_{Max} is the maximum power and $V_{O.C.}$ is the open-circuit voltage.

To visualize the amount of power produced by the generator, an incandescent light bulb bank was fabricated. The light bulb bank was wired in parallel and could accommodate up to 24 individual 14 V, 4.9 W light bulbs. To account for voltage uncertainty of the generator, the bulbs were tested to estimate maximum voltage before failure, which occurred around 32 volts.

In addition, every 500 milliseconds, the CBT software documented the voltage differential across each couple, as well as the overall voltage change across each module. A visual couple status indicator was created to display the status of each couple in the generator. Couples that performed above the voltage threshold were indicated by a green light and couples that had fallen below the voltage threshold were indicated by a red light. A counter was implemented in both data acquisition systems to enable synchronized data comparison between the two systems.

The final generator assembly can be seen in Figure 5-5.

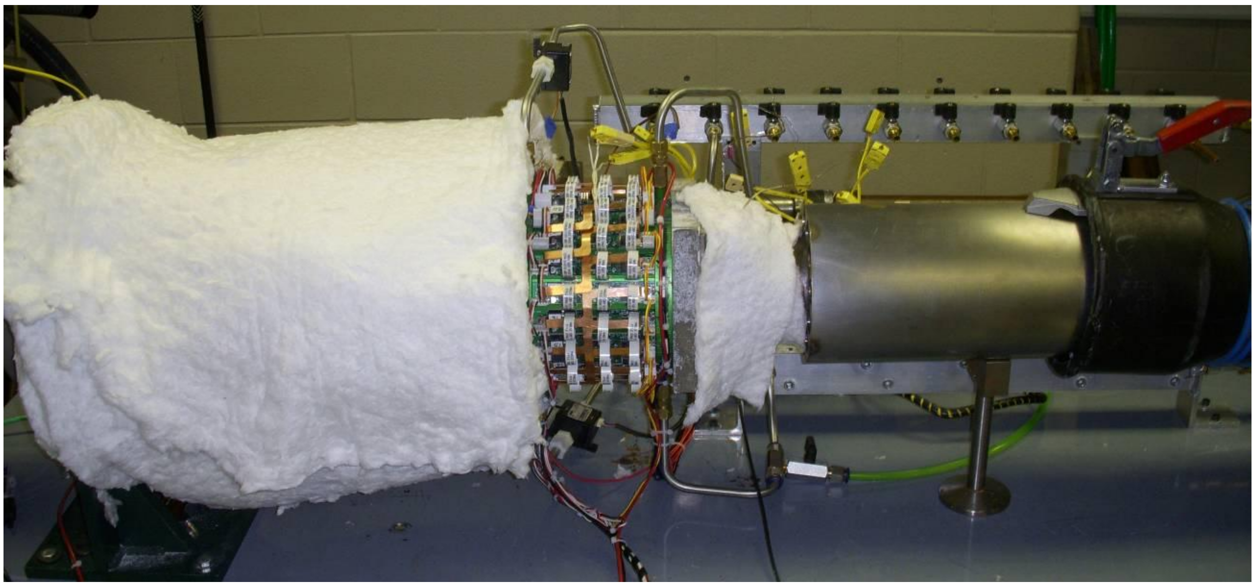

Figure 5-5 Completed 100 W Test Setup

5.2. Testing Process

Up to this point, the processes described have reflected current fabrication and assembly procedures. The following describes the process used during the 100 W test:

1. Attach building exhaust hose to the vented exhauster and turn on the pump
2. Set nitrogen flow rate to 12 CFM
3. Set chiller temperature to -6°C and coolant flow rate to ≈ 8 liters/min
4. Begin recording measurements from data acquisition system

5. Begin continuous monitoring and testing of the CBT via the supervisory controller
6. Ramp Airtorch temperature up to 925°C over 30 minutes
7. Once Airtorch is at temperature, increase nitrogen flow rate to maximum possible while maintaining Airtorch temperature ≥ 915°C; adjust chiller temperature if necessary
8. Measure generator open-circuit voltage and divide by 2 to estimate maximum power voltage
9. Back load generator with power supply at current levels above and below maximum power voltage estimation to calculate maximum generator power
10. Use maximum power values obtained in step 8 to determine the number of light bulbs needed for light bulb bank
11. Load generator with light bulb bank and photograph
12. Ramp Airtorch temperature down to room temperature in 30 minutes
13. After generator temperature has fallen below 75°C, close nitrogen flow
14. Stop recording measurements from data acquisition system
15. Turn off chiller
16. Turn off building exhaust hose pump

5.3. Post-processing Data

As with previous tests, the data collected from the 100 W test were compiled and post-processed to obtain the following information:

- Power Levels
    - As power generation is the main function of the TEG, one of the most important post-test calculations is the amount of power that was produced by the generator

- Steady-state hot side and cold side temperatures
    - Calculating these temperatures allows evaluation of the effectiveness of different TED insulation types and generator insulation
    - This calculation can also help assess how realistic the test was by comparing these values to known exhaust temperature values for target engines.

- Maximum and average ΔT
    - As the power generation of TEDs is a function of ΔT, it is necessary to obtain these values to normalize performance

- Heat transfer
    - Calculating the amount of heat transferred through the TEDs is necessary to calculate thermal efficiency
    - Calculating the heat transfer of the nitrogen gas and the cooling fluid allows an evaluation of the TED insulation

- Module voltage
    - Establishing a relationship between voltage production and ΔT is critical to determine optimal operating temperatures
    - Module voltage data can also pinpoint couple breakage times, helping to establish relationships between environmental conditions and couple failures

One of the most important post-processing operations is calculating the thermal efficiency of the TEG. Thermal efficiency is defined as the useful energy output of a device divided by the energy input. Knowing the thermal efficiency of the TEDs allows for a normalized performance comparison between different thermoelectric materials and aids in predicting the level of energy recovery possible by implementing TE technology with existing processes.

To calculate the thermal efficiency of the generator, the mass flow rate and the inlet and outlet temperatures of the cooling water are used to calculate the rate of heat transfer to the water. Assuming that a negligible amount of heat transfer occurs across the aerogel insulation, all of the heat gained by the water must pass through the legs of the TE couples. Dividing the electrical energy production rate of the generator (the useful energy output) by the rate of heat transfer to the water plus the electrical production rate of the generator (the energy input) gives the thermal efficiency of the TEDs. Previous TEG designs have yielded thermal efficiencies of about 4%.

5.4. Summary

The testing process for the TEDs is accomplished by assembling the modules into a round generator and heating the hot sides of the TE couples with nitrogen gas via jet impingement. Concurrently, the cold sides of the TE couples are actively cooled with a propylene glycol-water mixture. This provides the ΔT necessary for the couples to generate a voltage and allow testing of the TEG. The testing process follows a standardized procedure to measure maximum power generation and temperature values. A vast network of instrumentation for data acquisition is used to measure and calculate these values. A standardized method of data post-processing provides calculations such as average ΔT and thermal efficiency.

Chapter 6

6. Results & Discussion

The previous 100 W generator tests were performed with TEDs made up of legs with twice the cross-sectional area of the legs used in the test described above. While the greater cross-sectional area of these legs allowed greater current flow and thus greater power generation per leg, it also increased hot-side interface stresses due to thermal expansion, resulting in material breakage during testing (see section 2.2). This material breakage prevented the generator from producing the targeted 100 W. The cross-sectional area of the legs used in this test was reduced for the two-fold purpose of lowering the current to a more practical value and more importantly, to reduce the thermal stresses during operation in order to prevent material breaks at the hot-side interface.

As described in section 2.2, two single-cycle tests of 1 module each and one dual-cycle test of 2 modules were conducted prior to the 20-module, 100 W test to assess the material integrity of the smaller leg size. None of the couples broke during these tests, seemingly indicating lower levels of thermal stress. Apart from the brazing agent used and the number of couples tested, the only major deviation from these tests that was made for the 100 W test was the use of Aerogel insulation with mica film inserts instead of Durablanket. Thus, similar success rates were anticipated for the 100 W test.

6.1. Power Results

As the test process was initiated, it was noted that two couples had already failed and had been automatically bypassed via the EASs. It was concluded that these couples likely broke during generator installation. As the generator continued to heat up, more couples failed. By the time the hot shoes had reached 450°C, the CBT was reporting that over half the couples had already broken. This unexpected mass couple failure made it impossible to realize the goal of producing 100 W. In addition, voltage measurements for some of the modules had railed to various values, eliminating the opportunity to accurately measure power generation. Thus, the power measurement steps were omitted and the cool down process was initiated.

After the test, 156 of the 200 couples were found to have a least one broken leg. Of those 156 broken couples, 155 had a broken P-type leg and 8 had a broken N-type leg. All leg breakages occurred at the hot side skutterudite and metallization layer interface.

6.2. CBT Results

During the test, it was unclear how the CBT was performing. The visual couple status indicator was displaying a much higher number of broken couples than was expected and the displayed module voltages were different than the sum of the displayed voltages across their individual couples. It was determined after the test that this discrepancy was caused by a difference in the methods used by the microcontrollers to measure the voltage differential across individual couples and to measure the voltage change across the modules. In addition, an inside trace failed on module 4 which severed the communication to the entire module and railed the measured voltage differential for each couple in that module to a value above the fail threshold.

As the generator was cooling down, a picture was taken of the visual couple status indicator just before the CBT control system was shut down (Figure 6-1). According to the indicator, 140 couples had fallen below the voltage threshold and therefore had at least one broken leg. After the generator was disassembled, 156 couples were found to have broken legs. Figure 6-2 displaces a grid showing the actual leg status of each couple.

Figure 6-1 TE Couple Status as Predicted by CBT

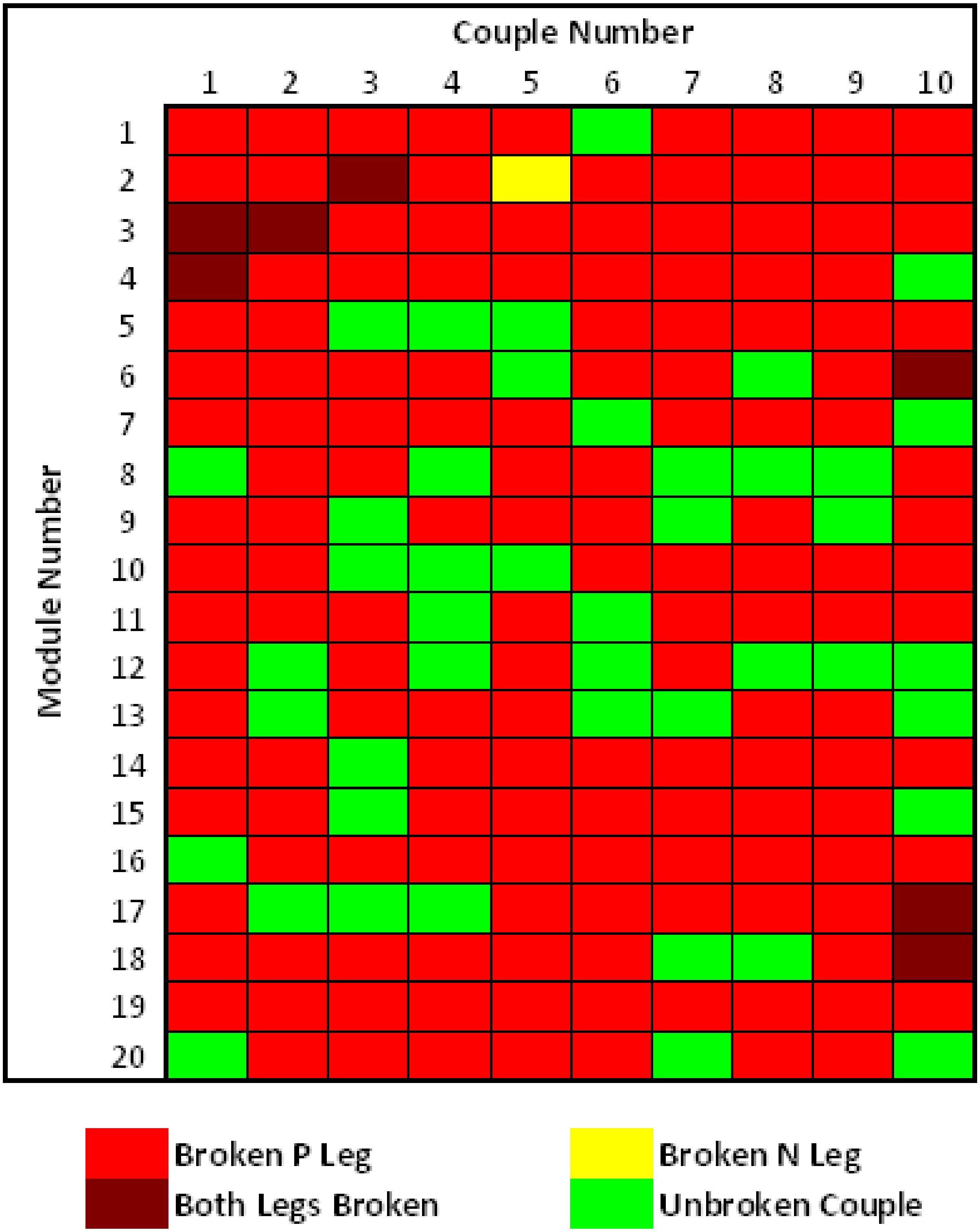

Figure 6-2 Post-Test Leg Status

All of the couples that were predicted by the indicator to have broken legs were found to have at least one broken leg. In addition, 16 couples that were predicted by the indicator to have no broken legs were found to have at least one broken leg. This discrepancy is likely due to the fact that the CBT software was deactivated before the generator had finished cooling. As the hot shoes of the couples were still around 400°C when the picture was taken, it is quite possible that the leg breakages in the 16 couples that were incorrectly predicted to have no broken legs occurred after the picture was taken, either while the generator was cooling, or during generator disassembly. This is supported by the fact that no couples that were found to be unbroken were incorrectly predicted by the indicator to have broken legs. In the best case scenario, the CBT correctly predicted the integrity status of 100% of the couples, assuming that each of the 16 incorrectly predicted couples broke after the picture was taken and excluding module 4, which lost communication. In the worst case scenario, the CBT correctly predicted the integrity status of 91.6% of the couples, assuming that each of the 16 incorrectly predicted couples broke before the picture was taken and excluding module 4. Figure 6-3 displays a grid showing the indicator's predicted status and the actual status of each couple

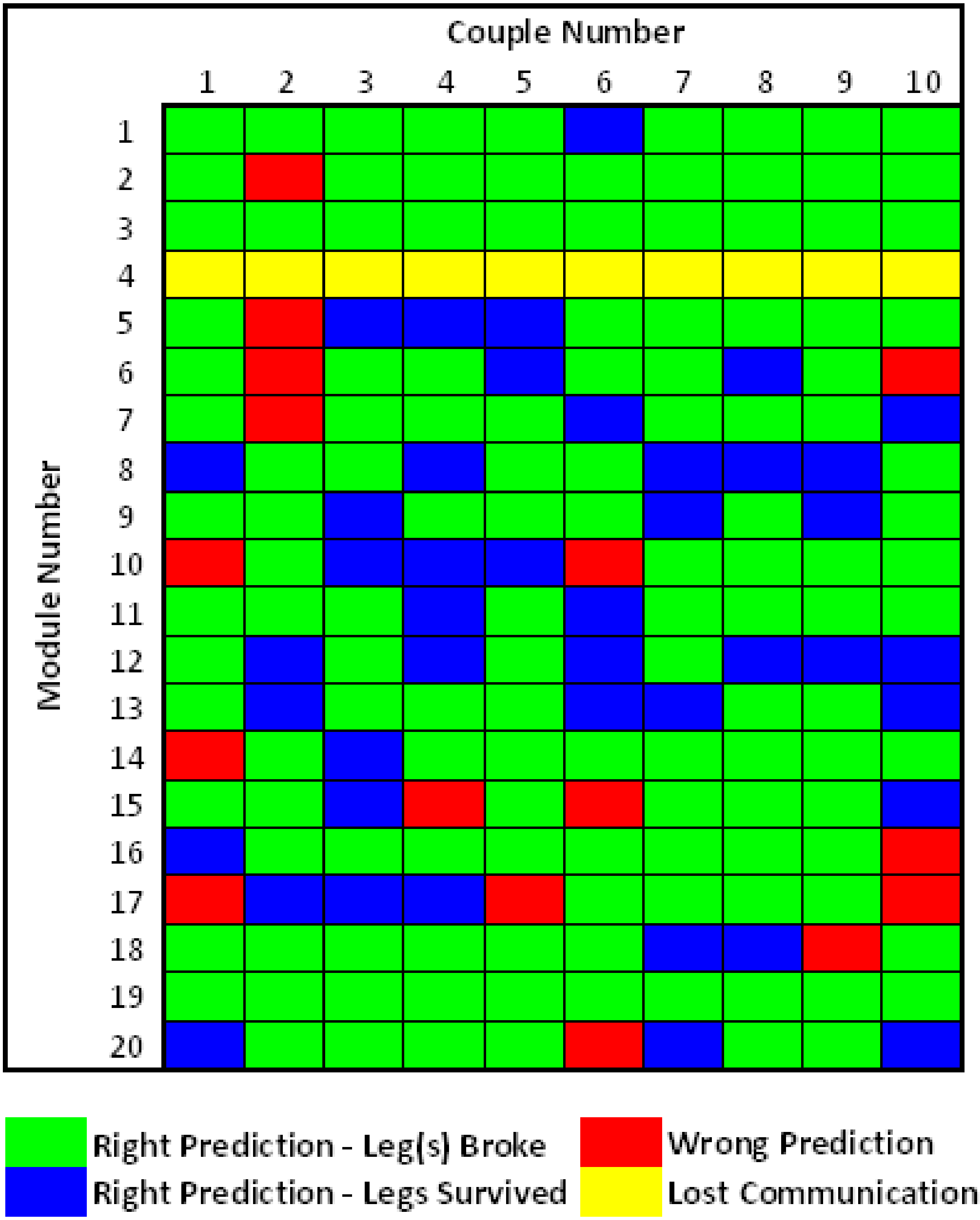

Figure 6-3 CBT Prediction Accuracy

6.3. Insulation Comparison Test

As the insulation type and brazing agent used were the only major changes that were made from the earlier generator tests that had 100% couple success rates, another test was performed to evaluate the effect of insulation type on couple structural integrity. Another 3 modules were fabricated from TE material similar to what was used in the 100 W test. One module was insulated with aerogel and a mica film, another was insulated with just aerogel and the third was insulated with Durablanket, the type of insulation used in the previous 2-module tests (Figure 6-4).

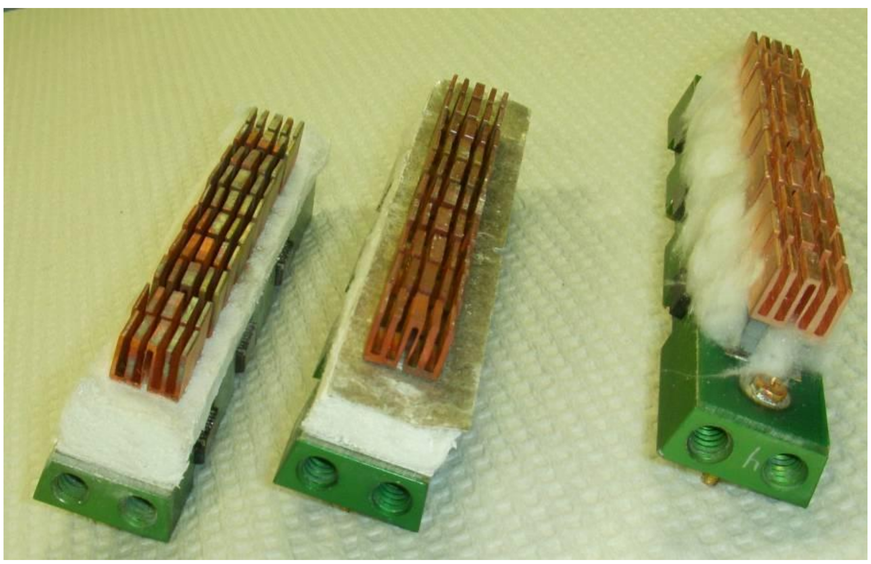

Figure 6-4 Modules Used in Insulation Comparison Test

6.3.1. Test Setup

As many variables as possible were left unchanged for the insulation comparison test. Similar TE material was used, the same bonding process and module assembly methods were used and the same CBT setup and control procedures were used. As the 17 modules not being tested were needed to complete the generator framework, they were included in the test as well but were not connected to the microprocessor boards, power, or load. Including these 17 modules in the insulation comparison test also helped to reduce variability from the 100 W test.

One significant deviation from the previous test was the way in which power was measured. The three modules were not wired in series as in the previous test; instead, each module was connected to a separate load. During the 100 W test, as well as most of the tests before it, the modules were back loaded with a Kepco power supply at incremental current levels and the corresponding generator voltages were measured to calculate the generated power. For this test, power was measured by sequentially loading each individual module with a 3 level resistor bank: 0.11 ohms, 0.44 ohms and 0.77 ohms. The current was measured for each of these resistance levels and power generation was calculated using the common relation: $P = VI$.

The testing procedure was similar to that of the 100 W test, but with a different method of calculating power generation. The light bulb visualization was not used either, as the purpose of this test was not total power generation, but insulation comparison. Additional thermocouples were installed in the hot and cold shoes of the center couple in each module to measure the variation of ΔT between the different insulation types. The three modules being tested were spaced in the generator such that each test module had a non-tested "dummy" module on each side. The modules were placed in the following order: Durablanket-insulated module, dummy module, aerogel-and-mica-insulated module, dummy module, aerogel-only-insulated module. The three modules being tested were connected to their respective microprocessor boards and the CBT supervisory control software was modified to accommodate 3 modules, instead of 20.

6.3.2. Results

The voltage measurements for the insulation comparison test provide an insightful look at the effect of CBT on module voltage over the duration of the test. For the beginning portion of the test, the voltages for all three modules steadily rose as the copper hot shoes climbed to a temperature of about 420-450°C. As seen in Figure 6-5, the voltages of the two modules with aerogel insulation peaked and started to decline after 1600 seconds. As there was a steady external resistance of 0.11 ohms on the generator during this portion of the test, this voltage drop was due to an increase of internal resistance in one or more of the thermoelectric legs, an indication of gradually failing structural integrity. Recall that the CBT software is written such that once a couple reaches a certain negative voltage for a specified amount of time, the corresponding EAS is closed, giving the circuit a low-resistance path in parallel with the failing couple. The sharp voltage jumps in the graph indicate EAS activation times for the module. The sharp increase in voltage occurs since the module current is no longer forced to pass through the high resistance legs of the failing couple, but can instead pass through the low-resistance EAS.

As the generator was heating up, it was discovered that one of the couples in the Durablanket-insulated module was already broken. It is likely that this break occurred during generator assembly. After the hot shoes reached a temperature of about 420-450°C, 7 couples in the aerogel-only insulated module broke, while 8 couples in the aerogel-and-mica insulated module broke. During the cool down portion of the test (not shown in Figure 6-5), 1 couple in the Durablanket-insulated module broke. Thus, over the entire test, the module with Durablanket insulation had only one couple break that was not broken before the test began.

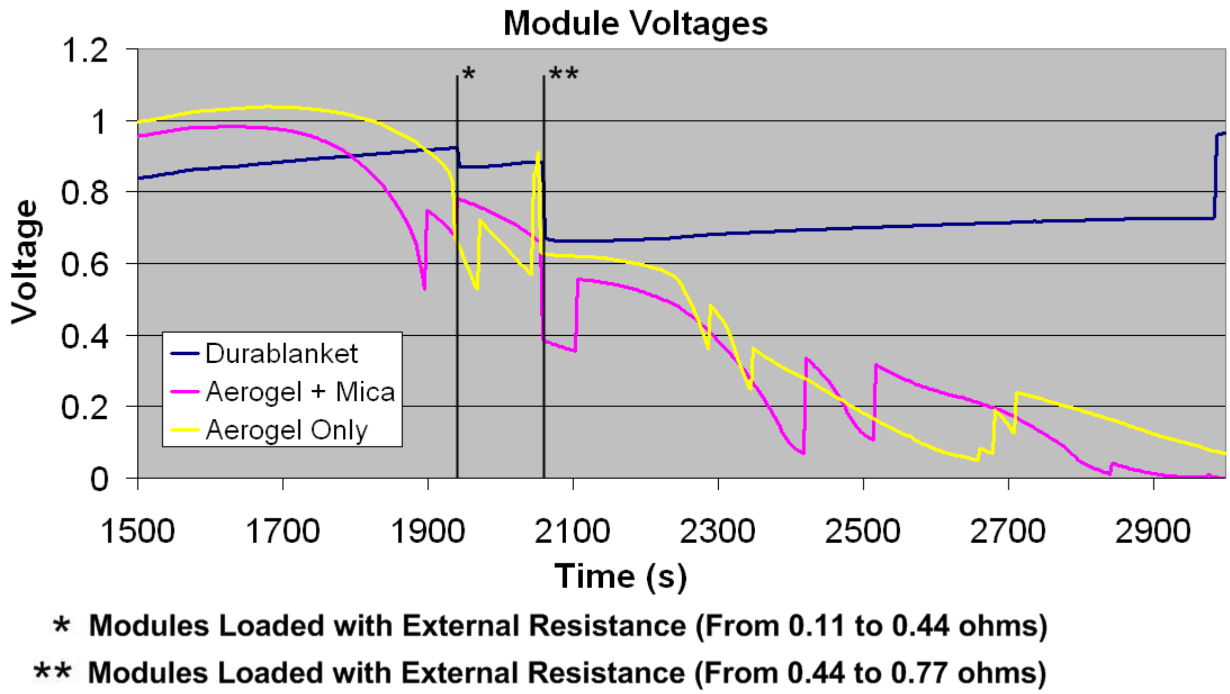

Figure 6-5 Module Voltages during Insulation Comparison Test

While the modules that were insulated with aerogel experienced much higher couple failure rates than the module insulated with Durablanket, it is doubtful that the insulation materials themselves are responsible for the breakages. Instead, it is likely that the insulation type directly affects additional variables that in turn, directly affect the thermal stress on the couples. While these additional variables are still unknown, there seems to be a correlation between temperature and couple failures. As seen in Table 6-1, the modules that were insulated with aerogel experienced significantly higher hot side temperatures and maximum ΔT values than the module insulated with Durablanket.

Table 6-1 Maximum ΔT and Hot Side Temperatures for Insulation Comparison Test

Insulation Type	Number of Broken Couples	Max ΔT (°C)	Max Hot Side Temp (°C)
Durablanket	2	446	481
A Only	7	509	535
A+M	8	513	533

6.4. Individual Couple Testing Results

Couples that were individually tested (see section 3.3.3) had a ΔT of about 600°C and produced an average of ≈ 1 W. This is almost twice the power produced from the average couple with similar ΔT values tested in the generator. One reason for this discrepancy is the higher resistances that accumulate when combining couples into modules. However, electrical resistance measurements of modules are typically only 10-20% higher than the sum of the electrical resistance measurements of the couples in the module. In addition, none of the 18 couples that were cycled in the individual couple test stand failed, or even suffered moderate degradation. Thus, it has been theorized that the compression experienced by the TE couples during the individual couple testing procedure may help improve power output and material integrity.

6.5. Summary

During the 100 W test, over 75% of the TE couples failed, increasing the difficulty and nullifying the usefulness of any power calculations. After the test, it was discovered that 155 P-type legs had broken and 8 N-type legs had broken, all at the hot side skutterudite and metallization layer interface. As the most significant design change from the previous, smaller and highly successful generator tests was the insulation type, another test was conducted with 3 modules, each with a different insulation type. The two modules that were insulated similar to the modules of the 100 W test had a 75% couple failure rate, while the module that was insulated similar to the smaller tests had an 11% failure rate during the test. However, the two modules that were insulated similar to the modules of the 100 W test had a significantly higher maximum ΔT and hot side temperatures than those of the module insulated similar to the smaller tests. Further investigation is needed to determine the true cause of the couple breakages.

Chapter 7

7. Conclusions

The experiments that are performed early on in a research area are rarely conducted without a few unexpected results. Further investigation of these apparent "anomalies" can often lead to new discoveries and a better understanding of the science involved. As Richard Buckminster Fuller noted, "There is no such thing as a failed experiment, only experiments with unexpected outcomes" [22]. Thus, while the 100 W test may not have reached the stated goal of producing 100 W, there are other results and discoveries that we can learn from these "unexpected outcomes."

7.1. Research Achievements

- A procedure for generator fabrication, assembly and testing has been established. This procedure provides a method to accomplish the following tasks in a standardized, repeatable manner:
    - Material Synthesis
    - Leg Fabrication
    - Bonding Process
    - Module Formation
    - CBT Integration
    - Generator Assembly and Testing

- A tracking system has been established. This system can be used to track an individual leg from its location in the hot-pressed ingot to its eventual position in the TEG. This facilitates the opportunity to evaluate the effect that various, adjustable parameters have on TE performance.

- The CBT has been successfully tested with supervisory control. The system was able to accurately detect couple failures and successfully establish a low-resistance path through EASs in parallel with the failed couples to maintain the closed-loop circuit and thus, overall power generation.

- A possible correlation between insulation type and couple structural integrity has been discovered. Current observations and assumptions suggest that a module's insulation type likely affects a third variable (such as ΔT) which in turn, directly affects the structural integrity of the couples in that module.

7.2. Conclusions of Research

From the outcomes of these generator tests and those previously conducted, a number of conclusions can be drawn regarding the optimal performance of TE generators.

Couple Bypass Technology

Until skutterudite material advancements are made such that the number of couple failures becomes insignificant, a method of bypassing failed couples will be necessary to measure series power generation. Even after such advancements are made, a module bypass system will likely be needed in any practical implementation of TE technology to mitigate the effects of a broken couple and allow power production for the rest of the generator until repairs can be made. The CBT tested in these experiments has shown great potential to meet these bypass requirements and should be included in future generator tests to further evaluate and improve the accuracy and automation of the technology. After material advancements are made, the CBT can be easily modified to monitor and bypass on a module level, rather than a couple level.

Couple Failures

The single greatest roadblock currently facing skutterudite research is the high level of thermal stresses at the interface between the hot shoe and the skutterudite. Each of the observed failures occurred between the skutterudite and the upper metallization layer: Material B for the P-type and Material A for the N-type. While these thermal stresses compromise the structural integrity of both N-type and P-type legs, the failure rate of the P-type legs was significantly higher than that of the N-type leg. Thus, it is logical to assume that the composition of the metallization layers also affects the structural integrity of the legs. The high failure rate observed in these tests must be addressed in order for TE generators to be feasible for practical application.

7.3. Recommendations for Future Work

While much work remains in TE research, efforts made in the following areas will build on the framework already established and provide additional insight into the results of these tests.

Couple Bypass Technology

As described above, the CBT tested in these experiments has shown great potential to meet the bypass requirements necessary to test multiple modules wired in series without jeopardizing overall power generation. To further develop this useful technology, additional testing and improvements should be made that focus on automatic control. Up to this point, all CBT testing has featured supervisory control which included manual resetting of the EASs. Testing the automatic mode of the CBT would be useful to either validate the current system, or to expose any programming errors or system bugs. Additionally, the discrepancy between reported module voltages and the sum of the reported individual couple voltages warrants a closer look at the two different methods used by the microcontroller to make these measurements. Testing will be needed to assess the accuracy of each method. Following these tests, design changes may be necessary to improve the accuracy of one or both methods. Efforts should also be made to condense the hardware currently populated on two separate boards onto one control board. This would eliminate the ribbon cables and accompanying connectors as well as the losses and vulnerabilities associated with them. Finally, as the CBT was developed and integrated after the round generator design was implemented, it has been suggested that a new generator design could be developed that takes CBT thermal conditioning and spacing needs into account from the very beginning.

Insulation Effect

The results of the insulation comparison test seemingly indicate a correlation between insulation type and couple breakages. This correlation is likely due to a third variable affected by the insulation type, such as ΔT or hot side temperature. Additional tests should be conducted to verify the findings of the insulation comparison test and investigate possible causes of the couple breakages in order to determine methods of reducing the number of these failures.

Brazing agents

The high success rates of the previous generator tests of this leg size conflict with the low success rates of the generator tests discussed in this Thesis. As mentioned before, the only major deviations from the previous generator tests were the insulation type and the brazing agent. Preliminary results from the insulation comparison test seem to indicate a correlation between insulation type and couple success rates. However, it would also be insightful to run a side-by-side brazing agent comparison test to investigate the effect of the different brazing agents on couple success rates. While the failures occur at the metallization layers rather than the leg and hot shoe interface, the uncertainty of the physical and chemical reactions that occur at high temperatures warrant an investigation of the effect of the brazing agent on couple integrity.

Leg Cross-Sectional Area

The level of thermal stresses experienced by the TE legs during testing is a function of the cross-sectional area of the legs. FEA studies of the interface of the skutterudite and metallization layers indicate that legs with larger cross-sectional areas experience higher levels of stress caused by thermal expansion [23]. While these studies have already prompted the reduction of the TE leg size (see section 2.2), a further reduction of the leg size could reduce the levels of thermal stress even further, improving leg survival rates. This reduction in leg size is not without disadvantages, however. The amount of current a leg produces for a given load is proportional to the cross-sectional area. Thus, for a given voltage, a leg with a larger cross-sectional area will produce higher current, and thus greater power, than a leg with a smaller cross-sectional area. To achieve similar power levels then, a greater number of smaller cross-sectional area legs is needed, which increases couple fabrication cost and time. Additional tests should be conducted to evaluate the success rates of legs with smaller cross-sectional areas. This will aid in determining if the reduction in thermal stresses gained by reducing the cross-sectional area of the leg size outweighs the increase in fabrication cost and time.

Compression Testing

While the success rates of the generator tests vary, the success rates of the individual couple testing (described in section 3.3.3) are consistently 100%, even after multiple cycles. In addition, the power produced by the average couple during individual couple testing is about twice the power produced by the average couple during generator testing. One of the main differences between the generator tests and the individual couple tests is the method of heat transfer. The generator tests rely on forced convection via jet impingement, while the individual couple test uses direct conduction, which places the couple being tested under compression. It has been hypothesized that the greater power values and high success rates of the individual couple testing may be a result of this compression. Two options for testing these theories have been proposed:

- The generator test setup could be modified to place the couples under compression during testing

- The individual couple test stand could be modified to use jet impingement instead of direct conduction as the method of heat transfer

7.4. Summary

The research questions posed in chapter two:

- Is the current skutterudite thermoelectric generator design able to reliably achieve a power level of 100 W? If not, what roadblocks need to be overcome to consistently achieve this power level?
    - The high level of thermal stresses at the skutterudite and Material B interface compromises the integrity of the P-type leg during operation. The resulting breakages in the P-type legs are the single greatest roadblock to consistently producing higher power levels in skutterudite TEGs. While the current generator design is fully capable of achieving 100 W, attaining this power level consistently will require design improvements that drastically reduce the thermal stresses at the skutterudite and metallization layers in the legs.

- Can couple failures be accurately and reliable detected and bypassed to allow thermoelectric generators to be wired in series?
    - Preliminary results from the CBT tested in these experiments indicate that the technology is fully capable of bypassing broken couples when operated under supervisory control. Additional testing will be needed to assess the automatic control capabilities and the measurement accuracy of the technology. In addition, compiling the hardware onto a single board would ease fabrication and assembly efforts and improve module durability. However, the CBT shows great promise in fulfilling the bypass requirements for current and future skutterudite TEGs.

REFERENCES

REFERENCES

[1] J. Sakamoto, H. Schock, T. Caillat, J. P. Fleurial, R. Maloney, M. Lyle, T. Ruckle, E. Timm, L. Zhang, “Skutterudite-based thermoelectric technology for waste heat recovery: Progress towards a 1kW generator,” submitted to *Science of Materials: Special Edition on Thermoelectrics*, Dec, 2010, accepted Feb, 2011, pp. 2-3, 11*

[2] Yunus A. Cengel and Michael A. Boles, *Thermodynamics: An Engineering Approach*, 6th Ed, McGraw-Hill, New York, NY, 2008, p 650-651

[3] Caltech, “Brief History of Thermoelectrics,” http://www.thermoelectrics.caltech.edu/history_page.htm, (accessed March 25, 2011)

[4] J. Sakamoto, et al, “Skutterudite-based thermoelectric technology for waste heat recovery,” p. 3*

[5] G. L. Bennett, “Space Application,” In *CRC Handbook of Thermoelectrics*, ed. D.M. Rowe, CRC Press LLC, Boca Raton, FL, 1995

[6] Robert D. Abelson, Tibor S. Balint, Kathryn E. Marshall, Heros Noravian, James E. Randolph, Celeste M. Satter, George R. Schmidt, James H. Shirley, “Enabling Exploration with Small Radioisotope Power Systems,” 2004, available from http://trs-new.jpl.nasa.gov/dspace/bitstream/2014/40856/1/04-10.pdf (accessed March 25, 2011)

[7] R.C. O’Brien, R.M. Ambrosi, N.P. Bannister, S.D. Howe, H.V. Atkinson, “Safe radioisotope thermoelectric generators and heat sources for space applications,” *Journal of Nuclear Materials* 377, Issue 3, (July 15 2008), pp. 506-521, available from http://www.sciencedirect.com/science?_ob=ArticleURL&_udi=B6TXN-4SCKRXJ-2&_user=1111158&_coverDate=07%2F15%2F2008&_rdoc=1&_fmt=high&_orig=gateway&_origin=gateway&_sort=d&_docanchor=&view=c&_searchStrId=1693536156&_rerunOrigin=google&_acct=C000051676&_version=1&_urlVersion=0&_userid=1111158&md5=1153b61c17e88f29e9b5f895ae238ca0&searchtype=a (accessed March 25, 2011)

[8] Harold Schock, Eldon Case, Tim Hogan, Mecouri Kanatzidis, John Miller, Jim Novak, Fang Peng, Edward Timm, Tom Shih, Bin Zhu, Thierry Caillat, Jeff Sakamoto, Wayne Eckerle, Todd Sheridan, Charles Cauchy, “Thermoelectric Conversion of Waste Heat to Electricity in an IC Engine Powered Vehicle: Phase 1 Final Report,” submitted to US Department of Energy, 2005, p. 5

[9] Ibid, p. 4

[10] Ibid, pp. 12-27

[11] Harold Schock, Eldon Case, Tim Hogan, Jeff Sakamoto, Fang Peng, Edward Timm, Trevor Ruckle, Jim Winkelman, Tom Shih, Mecouri Kanatzidis, Thierry Caillat, Jean-Pierre Fleurial, Christopher Nelson, "Thermoelectric Conversion of Waste Heat to Electricity in an IC Engine Powered Vehicle: Phase 2 Final Report," submitted to US Department of Energy, 2009, pp. 33-40

[12] Andreas Panayi, "Thermoelectric Module – Finite Element Analysis," Project Report, Thermoelectrics, Harold Schock, MSU, 2010

[13] Rama Venkatasubramanian, Edward Siivola, Thomas Colpitts, Brooks O'Quinn, "Thin-film thermoelectric devices with high room-temperature figures of merit," *Nature*, 413, 2001, pp. 597-602, available from
http://www.nextremethermal.com/media/pdf/Nature413597602October11%202001.pdf
(accessed March 25, 2011)

[14] J. Sakamoto, et al, "Skutterudite-based thermoelectric technology for waste heat recovery," p. 9*

[15] Ibid, p. 4*

[16] Ibid, pp. 12-13*

[17] Ibid, p. 5*

[18] K. Moran, "Use of shorting (switches) in the thermoelectric generator," Project Report, Thermoelectrics, Harold Schock, MSU, 2011, p. 4

[19] Ibid, p. 3

[20] Ibid, p. 8

[21] Harold Schock et al. "Thermoelectric Conversion of Waste Heat to Electricity in an IC Engine Powered Vehicle: Phase 1 Final Report," pp. 4, 13

[22] Thinkexist, "Richard Buckminster Fuller Quotes,"
http://thinkexist.com/quotation/there_is_no_such_thing_as_a_failed_experiment/185928.html,
(accessed March 25, 2011)

[23] Andreas Panayi, "Thermoelectric Module – Finite Element Analysis," pp. 5-10

*Represents internal page number of report. Article was accepted but not published at press time.